

Wnt-Ror signaling to SIA and SIB neurons directs anterior axon guidance and nerve ring placement in *C. elegans*

Jason R. Kennerdell^{1,2}, Richard D. Fetter³ and Cornelia I. Bargmann^{1,*}

Wnt signaling through Frizzled proteins guides posterior cells and axons in *C. elegans* into different spatial domains. Here we demonstrate an essential role for Wnt signaling through Ror tyrosine kinase homologs in the most prominent anterior neuropil, the nerve ring. A genetic screen uncovered *cwn-2*, the *C. elegans* homolog of Wnt5, as a regulator of nerve ring placement. In *cwn-2* mutants, all neuronal structures in and around the nerve ring are shifted to an abnormal anterior position. *cwn-2* is required at the time of nerve ring formation; it is expressed by cells posterior of the nerve ring, but its precise site of expression is not critical for its function. In nerve ring development, *cwn-2* acts primarily through the Wnt receptor CAM-1 (Ror), together with the Frizzled protein MIG-1, with parallel roles for the Frizzled protein CFZ-2. The identification of CAM-1 as a CWN-2 receptor contrasts with CAM-1 action as a non-receptor in other *C. elegans* Wnt pathways. Cell-specific rescue of *cam-1* and cell ablation experiments reveal a crucial role for the SIA and SIB neurons in positioning the nerve ring, linking Wnt signaling to specific cells that organize the anterior nervous system.

KEY WORDS: Axon guidance, *C. elegans*, Neuronal development, Wnt signaling

INTRODUCTION

Understanding how neuronal ganglia, axon bundles and synapses are organized to create the central nervous system is a problem of challenging scope. We are addressing this question in the *C. elegans* nerve ring, an axon bundle that is derived from over half of the animal's 302 neurons and can be regarded as its brain (White et al., 1986). Most synapses between neurons and many neuromuscular junctions are located in the nerve ring. Axonal processes enter the nerve ring at multiple positions, some directly and some following indirect trajectories through the amphid commissure and the ventral nerve cord.

The axon guidance receptor SAX-3/Robo has a dramatic effect on nerve ring formation, although its only known ligand, SLT-1, is less important. In *sax-3* mutants, the nerve ring is anteriorly misplaced and defasciculated into multiple axon bundles; in *slt-1* mutants, the nerve ring appears normal (Zallen et al., 1998; Hao et al., 2001). Mutations of UNC-6/Netrin and VAB-1/Eph receptors have milder effects on nerve ring organization: *unc-6* mutants have defects in ventral nerve ring axons and synapses (Colón-Ramos et al., 2007; Yoshimura et al., 2008), and *vab-1* mutants variably disrupt the amphid commissure (Hao et al., 2001; Zallen et al., 1999). UNC-6 is produced by ventral CEPsh glia in the nerve ring (Wadsworth et al., 1996), but CEPsh ablation causes a more severe defect than an *unc-6* mutation (Colón-Ramos et al., 2007; Yoshimura et al., 2008). The variable and overlapping effects of mutations and cell ablations suggest that our understanding of nerve ring development is incomplete.

Although best known for their effects on embryonic patterning and cell fate, secreted Wnt proteins also direct cell and axon guidance along the anterior-posterior axis by acting as attractants or repellents (Fradkin et al., 2005). In the *Drosophila* central nervous

system, Wnt5 on posterior axon commissures repels axons expressing the receptor tyrosine kinase-like (RTK) receptor Derailed (Yoshikawa et al., 2003). Similarly, mammalian Wnt5a is a repellent for corticospinal neurons that express the Derailed homolog Ryk (Keeble et al., 2006). Mammalian Wnt4 is an anterior attractant for commissural axons that express the multi-pass transmembrane protein frizzled 3 (Lyuksyutova et al., 2003). Frizzled proteins are the best-understood Wnt receptors, with many effects on developmental patterning. There are four Frizzled proteins in *C. elegans*, five in *Drosophila* and ten in humans, each activated by a subset of Wnts (Logan and Nusse, 2004) (www.treefam.org). Frizzled proteins can function alone or with co-receptors of the LRP5 family, which also bind Wnts (van Amerongen et al., 2008). In addition, two distinct classes of RTKs, Drl/Ryk proteins and Ror proteins, can bind Wnts and act as Wnt receptors. The response of a cell to Wnts is defined by its receptor complement and its differential signaling through pathways that regulate transcription, calcium, the cytoskeleton or cell polarity (Mikels and Nusse, 2006; van Amerongen et al., 2008).

In *C. elegans*, three of the five Wnt genes and two of the four Frizzled genes affect cell migration and axon outgrowth in the posterior body (Zinovyeva et al., 2008). The most posteriorly expressed Wnt, LIN-44, affects neuronal polarity, axon guidance and synapse formation in posterior neurons, acting in a repellent mode through the Frizzled protein LIN-17 (Goldstein et al., 2006; Hilliard and Bargmann, 2006; Pan et al., 2006; Prasad and Clark, 2006). Another posteriorly expressed Wnt, EGL-20, affects overlapping axons and multiple cell migrations; its receptors are LIN-17 and MIG-1, both Frizzled proteins (Pan et al., 2006; Whangbo and Kenyon, 1999). A Wnt in the central body, *cwn-1*, affects the posteriorly migrating CAN neuron and has minor roles in axon guidance (Zinovyeva and Forrester, 2005). In addition to their roles in axon guidance, these Wnts and Frizzled proteins affect posterior cell division, polarity and morphogenesis, but apparently do not affect the anterior nervous system (Gleason et al., 2006; Green et al., 2008a; Rocheleau et al., 1997).

Ror proteins are the least-studied of the Wnt receptors (Green et al., 2008b). In some respects, Rors function as typical RTKs, as binding of mammalian Wnt5a to Ror2 stimulates its kinase activity (Liu et al.,

¹Howard Hughes Medical Institute, Laboratory of Neural Circuits and Behavior, The Rockefeller University, New York, NY 10065, USA. ²Program in Biological Sciences, The University of California, San Francisco, CA 94143, USA. ³Howard Hughes Medical Institute, Janelia Farm Research Campus, Ashburn, VA 20147, USA.

* Author for correspondence (cori@mail.rockefeller.edu)

2008). However, Rors can also act as co-receptors with Frizzled proteins, and the *C. elegans* Ror2 homolog *cam-1* is something of a mystery. *cam-1* has effects on CAN neuronal migration that resemble those of Wnt mutants, and also affects Wnt-dependent vulval development and cell divisions (Forrester et al., 1999; Green et al., 2007; Zinovyeva and Forrester, 2005). However, CAM-1 has been suggested not to act as a Wnt receptor, for two reasons. First, deletion of the CAM-1 intracellular kinase domain, either in the endogenous locus or in rescuing transgenes, fails to eliminate its biological activity (Forrester et al., 2004; Kim and Forrester, 2003). Second, CAM-1 often acts genetically as a Wnt or Frizzled antagonist. For example, *cam-1(lf)* mutants mimic the effects of *egl-20* overexpression on HSN neuronal migration (Forrester et al., 2004). The effects of CAM-1 on vulval development appear consistent with Wnt inhibition, and this activity can be provided when CAM-1 is expressed as a secreted protein from various cells near the vulva (Green et al., 2007). Nonetheless, in one vulval cell type, the kinase domain is essential for CAM-1 function (Green et al., 2008a).

Here, we describe the isolation and characterization of mutations in *cwn-2*. In contrast to other Wnt mutants that act in the posterior body, *cwn-2* mutants have severe defects in the anterior nervous system. We show that CAM-1 is a likely receptor for CWN-2. Through genetic analysis of *cam-1* and cell ablation experiments, we have uncovered roles for the SIA and SIB neurons as organizers of nerve ring development.

MATERIALS AND METHODS

Strains and genetics

Nematodes were cultured by standard methods (Brenner, 1974). Experiments were performed at 25°C unless otherwise noted. Newly isolated mutations and deletions were outcrossed at least five times. Genotyping primers are provided in Table S1 in the supplementary material. The following mutations and integrated transgenes were used: LGI, *lin-17(n677)*, *mig-1(e1787)*, *lin-44(n1792)*, *mom-5(zu193)*; LGII, *cam-1(gm122)*, *cam-1(ks52)*, *cwn-1(ok546)*; LGIV, *cwn-2(ky736)*, *cwn-2(ky756)*, *cwn-2(ok895)*, *egl-20(n585)*, *ced-3(n1717)*; LGV, *cfz-2(ok1201)*, *akls3[nmr-1::gfp]*; LGX, *slt-1(eh15)*, *sax-3(ky200)*, *sax-3(ky123)*, *mig-13(mu225)*, *gmls18[ceh-23::gfp]*. A complete strain list is provided in Table S2 in the supplementary material.

Isolation and characterization of mutations

slt-1(eh15) gmls18 animals were mutagenized with ethyl methyl sulfonate as described (Epstein et al., 1995) and F2 progeny representing 1300 haploid genomes were screened for nerve ring phenotypes clonally at high magnification on a Zeiss Axioplan fluorescence microscope. The screen yielded two *cwn-2* mutants, *ky736* and *ky756*, and 15 other mutants. *cwn-2* mutants had defective nerve rings when crossed away from *slt-1*, and were characterized further as single mutants. *cwn-2(ky736)* was mapped to the region between *stP44* and *pkP4042* using Tc1 polymorphisms and SNP mapping with the strain CB4856. *ky736* was mapped to chromosome IV and failed to complement *ky736*. In *ky736* animals, a G-to-A mutation altered the splice donor of the third intron. In *ky756*, a G-to-A mutation in the third exon changed W155 to a stop (amber) codon.

The distortion of the head in *cwn-2* animals raised a concern that anterior structures might be poorly attached to each other, as observed in *lad-1* (LICAM), *sax-8/dig-1* and *zig-4* mutants (Aurelio et al., 2002; Benard et al., 2006; Sasakura et al., 2005). However, most attachment mutants do not have defects as L1 larvae, whereas *cwn-2* mutants do. In addition, *cwn-2* defects were stable over time in individual animals ($n=33$), whereas attachment defects typically increase with age (Zallen et al., 1999). By contrast, *cam-1(gm122)* nerve ring phenotypes change significantly in older larvae, suggesting a late secondary effect (see Fig. S1 in the supplementary material).

Electron microscopy

Newly hatched L1 animals of genotype *gmls18* and *cwn-2(ky756) gmls18* were prepared for electron microscopy, stained, and every fifth section was photographed as described (Adler et al., 2006). Serial sections were aligned

using ImageJ and corrected for artifacts using UnwarpJ. Renderings of serial reconstructions were made by tracing anatomical features using IMOD software (Kremer et al., 1996).

Microscopy

Nematodes were mounted in 2% agarose and anesthetized with 20 mM sodium azide. Confocal images with bright field were obtained using a Zeiss LSM510 microscope using a 100× (L1 stage) or 40× (L4 stage) objective. Projections of confocal stacks were made and merged using ImageJ. For DIC images to illustrate expression patterns, a Zeiss Imager.Z1 microscope was used. For nerve ring phenotype analysis, a Zeiss Axioplan II microscope was used with a 100× (L1 stage) or 20× (L4 stage) objective.

Transgenic rescue and cell ablation experiments

For all transgenes, results are representative of at least two strains with independent extrachromosomal arrays. Transgenic animals were scored at the L4 stage, except for *ceh-24::mig-1* and *ceh-24::egl-1*, which were scored at the L1 stage. Animals were scored for nerve ring phenotypes by an investigator blind to the presence of the transgene, which was scored subsequently based on the co-injection marker. In Fig. 3D and Fig. 6B, nerve ring defects in animals with the co-injection marker were normalized to internal control siblings lacking the marker, because in both *cwn-2* and *cam-1* rescued strains we observed some rescue of the nerve ring defect in these control siblings. This paradoxical rescue could result from maternal rescue, perdurance of early gene expression, or variable silencing of the co-injection marker. The normalization may skew quantification, but it was internally consistent with qualitative assessments of rescue in the same transgenic strains. For primary data, see Table S3 in the supplementary material.

ceh-24::egl-1 transgenes were generated and maintained in either a *ced-3(n1717)* or *ced-3(n1717) cwn-2(ky756)* mutant background to minimize lethality of the transgenes. They were crossed to either *gmls18*, *kyIs510* or *cwn-2(ky756) gmls18* and the resulting L1 animals were scored. In a *ced-3(+)* background, the transgene caused 20% embryonic lethality, presumably owing to *egl-1* killing of essential tissues (the *ceh-24* promoter is variably expressed in the intestine). To assay efficiency of cell killing, the *ceh-24::egl-1* transgene was introduced into a *ceh-24::GFP* strain; at least two *ceh-24*-expressing neurons were killed in 55% of the animals, but at least one neuron survived in all animals ($n=44$). Therefore, the nerve ring defect illustrated in Fig. 7 is a minimal estimate of the effect of killing SIA, SIB and SMD.

Heat-shock experiment

Eggs were collected from young adult *cwn-2(ok895) gmls18 kyEx1369* animals for 1 hour and transferred every hour for 12 hours at 15°C. After 11 hours, all plates were placed at 31°C for 1 hour, returned to 15°C, and scored for nerve ring defects at the L4 stage. Just prior to heat shock, eggs were examined to verify the embryonic stage.

Molecular biology

Standard molecular biology methods were used. For details of plasmid construction, see Table S4 in the supplementary material.

RESULTS

cwn-2 determines the placement of the developing nerve ring

Mutations that affect nerve ring development were identified in a sensitized genetic screen with a *ceh-23::GFP* sensory neuron reporter (see Materials and methods). This screen yielded two alleles of a gene subsequently identified as *cwn-2: ky736* and *ky756*. *cwn-2* mutants had anteriorly displaced nerve rings, a defect most easily observed by examining the relationship between the nerve ring and the pharynx. In wild-type animals, the nerve ring was centered around the isthmus of the pharynx (Fig. 1A,D); in *cwn-2* mutants, the nerve ring instead circled the metacarpus of the pharynx (Fig. 1B,E). *sax-3* mutants have a similar anterior nerve ring phenotype (Fig. 1C,F) and axon defasciculation that was not observed in *cwn-2* mutants (Zallen et al., 1998).

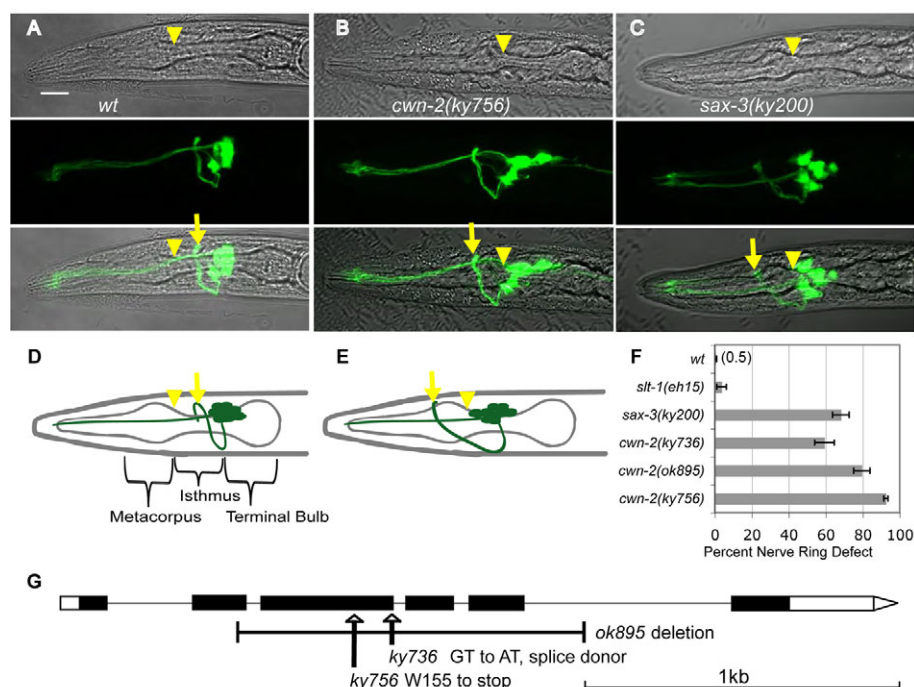


Fig. 1. Anterior displacement of the nerve ring in *cwn-2* and *sax-3* mutants.

(A–C) Confocal images of wild-type (*wt*), *cwn-2* and *sax-3* *C. elegans* L1 larvae expressing *ceh-23::GFP*. Top row, bright field; middle row, GFP projection; bottom row, merged image. Arrows indicate the position of the nerve ring, and arrowheads indicate the posterior boundary of the metacarpus. Anterior is left and dorsal is up. Scale bar: 10 μ m. (D) Diagram of wild-type pharynx and nerve ring. Dendrites extend anteriorly from the cell bodies. Sensory axons extend ventrally, then anteriorly, then dorsally into the nerve ring. (E) Diagram of an anteriorly displaced *cwn-2* nerve ring circling the metacarpus of the pharynx. (F) Quantification of nerve ring defects at the L1 stage. An animal was scored as defective if the nerve ring was as far anterior as the metacarpus (arrowhead in A–E). (G) Diagram of the *cwn-2* genomic region. Black boxes represent exons, white boxes represent untranslated regions, and lines represent introns. *cwn-2* lesions are indicated.

The mutant phenotypes were observed in over 75% of *cwn-2(ky756)* animals at all stages, from the first larval stage (L1) to the adult (Fig. 1F). Anterior nerve rings were evident in *cwn-2* mutants when sensory neurons were labeled with the fluorescent dye DiI, in the absence of the *ceh-23::GFP* reporter, or when interneurons were labeled with *nmr-1::GFP* (data not shown). These results suggest a broad defect in *cwn-2* nerve ring placement that is independent of the marker; unless otherwise stated, further experiments were conducted using *ceh-23::GFP*.

The *ky736* and *ky756* mutants were mapped to a small region on chromosome IV (see Materials and methods), and were rescued by a genomic DNA fragment containing the *cwn-2* gene. *ky756* mutants had a nonsense mutation in the third exon of *cwn-2*, and *ky736* had a mutation in the splice donor of the third intron (Fig. 1G). All alleles were recessive. *cwn-2(ok895)*, a deletion allele kindly provided by the *C. elegans* knockout project, resembled *ky756* (Fig. 1F); these molecular lesions and their similar severity suggest that *ky756* and *ok895* represent null alleles of *cwn-2*. The milder nerve ring defect in *ky736* suggests that it is a partial loss-of-function allele (Fig. 1F).

Neuronal tissues and some non-neuronal tissues shift coherently in a *cwn-2* mutant

To further characterize the anterior defect, the head of a *cwn-2* L1 larva and of a wild-type L1 larva were analyzed in serial-section transmission electron micrographs. Sections covering ~ 30 μ m, comprising the anterior $\sim 20\%$ of a newly hatched animal, were photographed at high magnification and the resulting images aligned and stacked to produce a three-dimensional representation of each animal. Tissues and cells of interest were manually traced and modeled using IMOD software (Kremer et al., 1996). As expected, the nerve ring was anteriorly misplaced in the *cwn-2* animal compared with the wild type, both in absolute terms and with respect to an internal reference tissue, the pharynx (Fig. 2). Neuronal cell bodies anterior and posterior of the nerve ring were anteriorly misplaced, but maintained near-normal positions with respect to

each other and the nerve ring (Fig. 2A,B). The amphid commissure, an axon bundle immediately posterior of the nerve ring, was also anteriorly positioned (Fig. 2C, yellow arrowheads). These changes reveal a general anterior shift of *cwn-2* neuronal tissues.

Several muscle and epithelial cells were also altered in the *cwn-2* animal. *C. elegans* head muscles send arms into the nerve ring, where they form neuromuscular junctions; the *cwn-2* muscle arms joined the nerve ring at its abnormal anterior position (Fig. 2D, red arrowheads). The excretory pore cell forms a duct to the exterior environment near the nerve ring; the duct was shifted anteriorly in the *cwn-2* mutant (Fig. 2C, green arrow). The isthmus of the *cwn-2* pharynx was slightly shorter and thicker than normal, but not sufficiently altered to explain the nerve ring displacement; head shape was slightly distorted, and the nuclei of epithelial cells and muscle cells were slightly disorganized in placement (Fig. 2A). All phenotypes were confirmed in live animals using GFP markers or Nomarski microscopy (data not shown). In summary, the electron microscopy analysis suggests that nerve ring misplacement is accompanied by the anterior misplacement of neuronal cell bodies, muscle arms and the excretory pore, and by a more normal placement of the internal structures of the pharynx and intestine.

cwn-2 acts during nerve ring formation, but need not be locally expressed

The expression pattern of *cwn-2* was examined by cloning a genomic fragment of *cwn-2* into a bicistronic expression vector with a GFP reporter (Coates and de Bono, 2002). At the comma stage of embryonic development when the nerve ring forms, *cwn-2::SL2::GFP* was expressed in the developing intestine and pharyngeal muscle, which are posterior to the developing nerve ring (Fig. 3A). The overall expression pattern was maintained in larval and adult stages, with *cwn-2::SL2::GFP* expression in intestine, pharynx, anterior body wall muscle, vulva and SMD head neurons (Fig. 3B,C). The *cwn-2* expression pattern is largely non-overlapping with the Wnts *cwn-1* (posterior muscles), *egl-20*

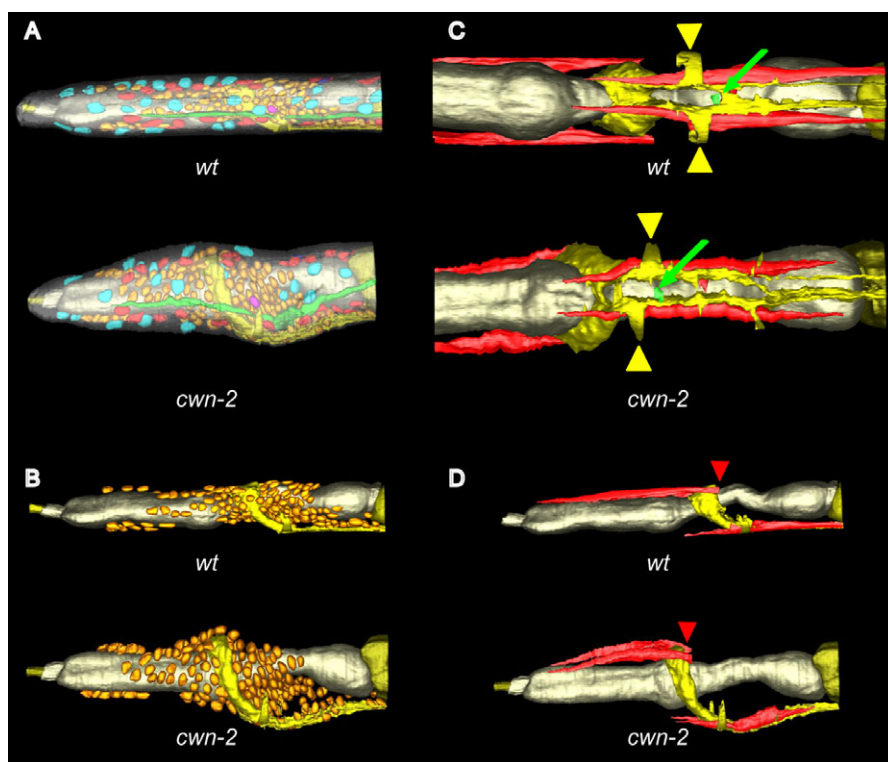


Fig. 2. Coherent mislocalization of the nervous system and associated structures in *cwn-2* mutants. (A–D) Renderings of wild-type and *cwn-2* *C. elegans* L1 larvae based on serial electron microscopy sections. (A,B,D) Lateral views; (C) ventral views. Off-white, perimeter of the worm; orange, neuronal nuclei; blue, epidermal nuclei; red, muscle; yellow, neuropil (nerve ring, ventral cords, amphid commissures); green, excretory canal and pore; gray, pharynx. (A) All tissues. (B) Renderings limited to nervous system and pharynx. (C) Renderings limited to neuropil, pharynx, excretory pore and select head muscles. Yellow arrowheads, amphid commissures; green arrow, excretory pore. (D) Renderings limited to neuropil, pharynx and select head muscles. Red arrowheads indicate termination points of muscle arms.

(epithelial cells of the tail and posterior body) and *lin-44* (tail epithelial cells) (see Fig. 8A) (Gleason et al., 2006; Herman et al., 1995; Pan et al., 2006; Whangbo and Kenyon, 1999).

To determine which tissues could provide *cwn-2* function for nerve ring development, a *cwn-2* cDNA was expressed in *cwn-2* mutants under the control of well-characterized promoters covering parts of its normal expression pattern. *cwn-2* expression in body wall muscles (*myo-3* promoter), pharynx (*myo-2* promoter) or intestine (*elt-2* promoter) rescued the nerve ring defects of *cwn-2* mutants, suggesting that the complete *cwn-2* expression pattern is not essential for nerve ring development (Fig. 3D).

The early *cwn-2*-expressing cells are posterior to the developing nerve ring, suggesting that *cwn-2* could provide an instructive posterior cue from any of these tissues. To test this idea, a *cwn-2* cDNA was expressed under the *slt-1* promoter, which is expressed in the most-anterior cells of the comma stage embryo (Hao et al., 2001). Surprisingly, anterior expression of *cwn-2* fully rescued *cwn-2* nerve ring defects (Fig. 3D), suggesting that *cwn-2* was equally active when expressed either anterior or posterior of the developing nerve ring.

The temporal requirement for *cwn-2* was defined by providing embryonic pulses of *cwn-2* from a broadly expressed heat-shock promoter. Heat-shock expression of *cwn-2* before

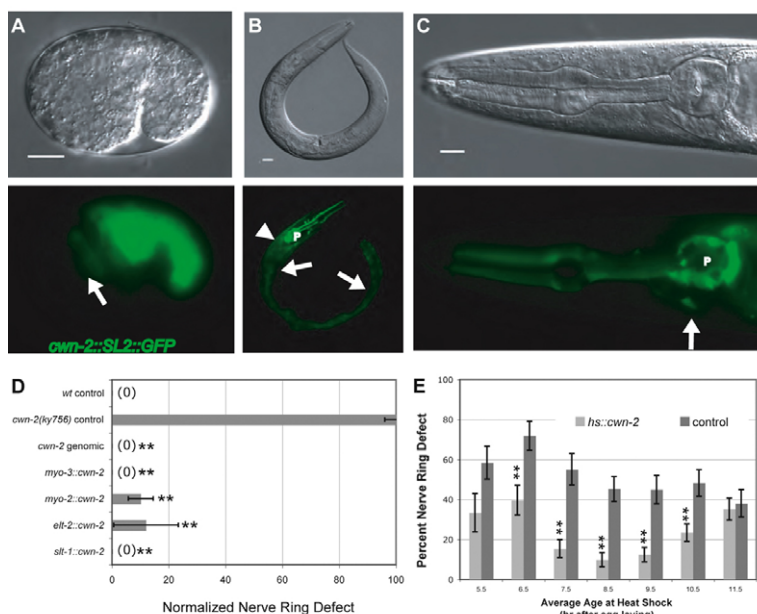


Fig. 3. Expression pattern and rescue of *cwn-2*. (A–C) DIC images (top) and GFP images (bottom) showing expression of *cwn-2::SL2::GFP*. (A) Comma stage *C. elegans* embryo. Arrow indicates approximate location of the developing nerve ring. (B) Adult. Arrowhead, body wall muscle; arrows, intestine; P, pharynx. (C) High magnification of adult head. Arrow, SMD neuron; P, pharynx. Scale bars: 10 μ m. (D) Transgenic rescue of *cwn-2* nerve ring defects by promoter::cDNA fusions. Nerve ring defects in each strain were scored at the L4 stage and normalized to defects in control siblings without the transgene (see Materials and methods). (E) Transgenic rescue of *cwn-2* nerve ring defects by embryonic heat shock-induced *cwn-2* expression. Controls are heat shocked *cwn-2* animals without the *hs::cwn-2* transgene. In D and E, error bars represent the s.e. of proportion. Asterisks indicate values different from controls at $P < 0.01$ by Student's *t*-test.

the comma stage resulted in substantial embryonic lethality (see Fig. S2 in the supplementary material), possibly owing to interference with embryonic Wnt patterning (Rocheleau et al., 1997). Heat shock near the comma stage (6.5–10.5 hours after egg-laying) resulted in significant rescue of the nerve ring defect and minimal lethality (Fig. 3E). Heat shock after the comma stage did not rescue nerve ring placement (Fig. 3E). These results suggest that *cwn-2* is required near the time of nerve ring development.

***cam-1*, *cfz-2* and *mig-1* encode candidate receptors that affect nerve ring development**

To identify receptors for *cwn-2* in nerve ring formation, we examined six candidate Wnt receptors: four encoded by the Frizzled genes *mig-1*, *lin-17*, *cfz-2* and *mom-5*, and two by the tyrosine kinase-like genes *cam-1*/Ror and *lin-18*/Ryk. The five receptors for which strong loss-of-function mutants are viable were examined using candidate null alleles. In the sixth case, the maternal-effect lethal *mom-5* mutant, we examined viable homozygous *mom-5* progeny from heterozygous mothers. Two receptor mutants, *cam-1* and *cfz-2*, had substantial anterior nerve ring defects as scored with the *ceh-23::GFP* sensory neuron marker (Fig. 4A,B); *lin-17*, *mig-1*, *mom-5* and *lin-18* mutants did not (Fig. 4B, Table 1). Both *cam-1* and *cfz-2* mutants had a well-organized, anteriorly displaced nerve ring, like *cwn-2* mutants (Fig. 4A). Nerve ring defects in *cfz-2* have been observed previously (Zinovyeva and Forrester, 2005). These observations suggest that *cam-1* or *cfz-2* could encode receptors for CWN-2.

If a ligand signals through a single receptor, a double mutant between null mutations in ligand and receptor should be no more severe than the worst single mutant. Matching this prediction, *cwn-2 cam-1* double mutants resembled *cwn-2* mutants; ~90% of the nerve rings were anteriorly displaced (Fig. 4B, Table 1). By contrast, *cwn-2 cfz-2* double mutants were enhanced compared with single mutants, as were *cam-1 cfz-2* double mutants, with 100% of the nerve rings anteriorly displaced (Fig. 4B, Table 1). Since predicted null mutations were used, these results suggest that *cfz-2* has some functions that are independent of *cwn-2* and *cam-1*, and vice versa. In the simplest interpretation, CAM-1 could be a receptor for CWN-2, and CFZ-2 could be a receptor for a second Wnt that functions in the nerve ring together with CWN-2.

There are several potential Wnt receptors in *C. elegans* and some might have redundant functions. To determine whether *mig-1* and *lin-17* could affect nerve ring development in sensitized genetic backgrounds, we tested them in double mutants with *cfz-2* mutations. *lin-17* did not enhance the defects of *cfz-2* mutations, but *mig-1 cfz-2* double mutants were more severe than either mutant alone (Fig. 4B, Table 1). *mig-1 cam-1* double mutants resembled *cam-1* single mutants (Fig. 4B, Table 1). The pattern of *mig-1* enhancement suggests that *mig-1* might function in the same pathway as *cwn-2* and *cam-1*.

The enhanced defects in *cwn-2 cfz-2* double mutants suggested that *cwn-2* might function with another Wnt in nerve ring development. Indeed, although *cwn-1* null mutants had minimal nerve ring defects, *cwn-2 cwn-1* double mutants were more severely affected than *cwn-2* (Fig. 4C, Table 1). A second Wnt mutant, *lin-44*, did not enhance *cwn-2* (Fig. 4C), and a triple Wnt mutant strain containing mutations in *egl-20*, *lin-44* and *cwn-1* was no more defective than any single mutant (Fig. 4C, Table 1). The embryonic lethal Wnt mutant *mom-2* was not tested. These results suggest that *cwn-1* plays a minor role in nerve ring development.

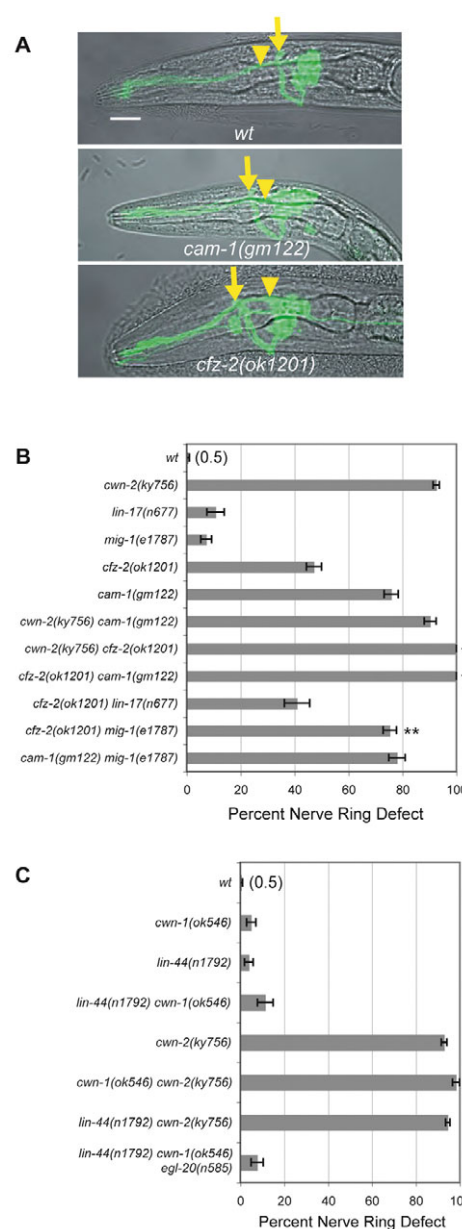


Fig. 4. Nerve ring defects in Wnt ligand and receptor mutants.

(A) Images of *C. elegans* L1 larvae illustrating anterior nerve rings in *cam-1* and *cfz-2* mutants. Images are confocal projections of *ceh-23::GFP* merged with a bright-field image. Arrows, nerve ring position; arrowheads, the posterior boundary of the metacarpus (as in Fig. 1). Anterior is left, dorsal is up. Scale bar: 10 μ m. (B) Nerve ring defects in *cwn-2*, candidate receptor, and double mutants at the L1 stage. (C) Nerve ring defects in Wnt mutants and double mutants at the L1 stage. In B and C, error bars represent the s.e. of proportion. Asterisks indicate double mutants different from either single mutant by Student's *t*-test or Fisher's exact test with Bonferroni correction. *, $P < 0.05$; **, $P < 0.01$.

***cam-1* may encode a receptor for CWN-2**

The intracellular domain of CAM-1 is unnecessary for many of its functions, suggesting that *cam-1* might encode an extracellular ligand or binding protein in the Wnt pathway (Francis et al., 2005; Green et al., 2007; Kim and Forrester, 2003). In agreement, *cam-1(ks2)* mutants lacking most of the predicted intracellular domain rarely had nerve ring defects, unlike *cam-1* null mutants (Fig. 5).

Table 1. Nerve ring defects in single and double mutants

Genotype	Anterior nerve ring (%)	<i>n</i>	<i>P</i> -value*
<i>wt</i>	0.5	204	
<i>slt-1(eh15) X</i>	3.7	54	
<i>sax-3(ky200) X</i>	68.2	110	
<i>cwn-2(ky736) IV</i>	59.3	86	
<i>cwn-2(ky756) IV</i>	92.5	523	
<i>cwn-2(ok895) IV</i>	79.5	83	
<i>cam-1(gm122) II</i>	75.8	265	
<i>cfz-2(ok1201) V</i>	47.2	318	
<i>mig-1(e1787) I</i>	7.3	165	
<i>lin-17(n677) I</i>	10.8	93	
<i>lin-18(e620) X</i>	1.8	109	
<i>mig-13(mu225) X</i>	2.0	100	
<i>mom-5(zu193) unc-13(e1091) I</i> (L4 stage using Dil)	0.0	23	
<i>cam-1(gm122) II; cwn-2(ky756) IV</i>	90.3	185	NS
<i>cwn-2(ky756) IV; cfz-2(ok1201) V</i>	100.0	100	<0.01
<i>mig-1(e1787) I; cfz-2(ok1201) V</i>	75.3	304	<0.005
<i>lin-17(n677) I; cfz-2(ok1201) V</i>	40.9	110	NS
<i>cam-1(gm122) II; cfz-2(ok1201) V</i>	100.0	66	<0.001
<i>mig-1(e1787) I; cam-1(gm122) II</i>	78.0	186	<0.005
<i>cam-1(ks52) II</i>	9.1	88	
<i>mig-1(e1787) I; cam-1(ks52) II</i>	27.1	107	<0.05
<i>lin-17(n677) I; cam-1(ks52) II</i>	27.2	81	<0.05
<i>lin-18(e620) X; cam-1(ks52) II</i>	3	100	NS
<i>cam-1(ks52) II; mig-13(mu225) X</i>	28.6	98	<0.01
<i>sax-3(ky200ts) X</i> at 20°C	9.2	109	
<i>cam-1(ks52) II; sax-3(ky200ts) X</i> at 20°C	64.0	100	<0.01
<i>cam-1(ks52) II; cfz-2(ok1201) V</i>	83.2	101	<0.01
<i>lin-44(n1792) I</i>	3.9	102	
<i>cwn-1(ok546) II</i>	5.0	100	
<i>lin-44(n1792) I; cwn-2(ky756) IV</i>	94.5	201	NS
<i>cwn-1(ok546) II; cwn-2(ky756) IV</i>	98.3	176	<0.05
<i>lin-44(n1792) I; cwn-1(ok546) II</i>	11.4	79	NS
<i>lin-44(n1792) I; cwn-1(ok546) II; egl-20(n585) V</i>	7.7	91	NS

Animals were scored at the L1 stage, unless otherwise noted. The *P*-value was calculated using Student's *t*-test or Fisher's exact test with Bonferroni correction for multiple comparisons. Animals were grown at 25°C unless otherwise noted.

*Double versus single mutants. NS, not significant.

It is becoming increasingly evident that Wnt receptors form multi-protein complexes with several signaling subunits (Lu et al., 2004; Tolwinski et al., 2003; Wehrli et al., 2000; Yamamoto et al., 2008; van Amerongen et al., 2008). The apparent dispensability of the CAM-1 intracellular domain could be explained if CAM-1 is part of a receptor complex, with some functional redundancy among receptor signaling domains. To test this idea, we asked whether sensitized backgrounds might unmask phenotypes for the intracellular deletion allele *cam-1(ks52)*. Partial loss-of-function mutations such as *cam-1(ks52)* might be enhanced by mutations in the same or different pathways, unlike null mutations (Guarente, 1993; Suzuki and Han, 2006). Beginning with other Wnt receptor genes, we found that *mig-1 cam-1(ks52)* or *lin-17 cam-1(ks52)* double mutants had stronger defects than either mutant alone, an enhancement not observed in *cam-1(null)* mutants (Fig. 5B, compare with Fig. 4B and Table 1). A *cfz-2* mutation was also enhanced by *cam-1(ks52)* (Fig. 5B), but a *lin-18* mutation was not enhanced (Table 1).

Two additional receptors of interest enhanced the weak *cam-1(ks52)* defect. *mig-13* has some similarity to mammalian LRP genes, which encode Wnt co-receptors (Sym et al., 1999; Wehrli et al., 2000). *mig-13* mutants did not have nerve ring defects, but *mig-13 cam-1(ks52)* double mutants had stronger defects than either mutant alone, suggesting a possible role for *mig-13* in Wnt signaling or in

another aspect of nerve ring development (Fig. 5B). Enhancement of *cam-1(ks52)* was also observed with the Robo temperature-sensitive mutation *sax-3(ky200)* at the partially permissive temperature of 20°C (Fig. 5B). Together, these results suggest that the CAM-1 intracellular domain has a function that overlaps with developmental roles of *mig-1*, *cfz-2*, *lin-17*, *mig-13* or *sax-3*.

We were concerned that *cam-1(ks52)* could have defects in mRNA or protein stability, so, as a complementary approach, we examined a highly expressed *cam-1::GFP* transgene with an intracellular domain deletion (Francis et al., 2005). This transgene efficiently rescued *cam-1(gm122)* null mutants and *cam-1 mig-1* mutants, but did not rescue the *cam-1 sax-3(ky200)* defect at 20°C (see Fig. S3 in the supplementary material). These results confirm a requirement for the intracellular domain of CAM-1 in one sensitized genetic background.

The SIA and SIB neurons may organize the nerve ring

If CAM-1 is an authentic CWN-2 receptor, its expression pattern could reveal cells important for nerve ring formation. *cam-1* has multiple splice forms encoded from three separate promoters (Fig. 6A) (Koga et al., 1999) (www.wormbase.org). To narrow down its activity, each *cam-1* cDNA was expressed from its cognate upstream sequence and introduced into *cam-1* null mutants. Rescue was

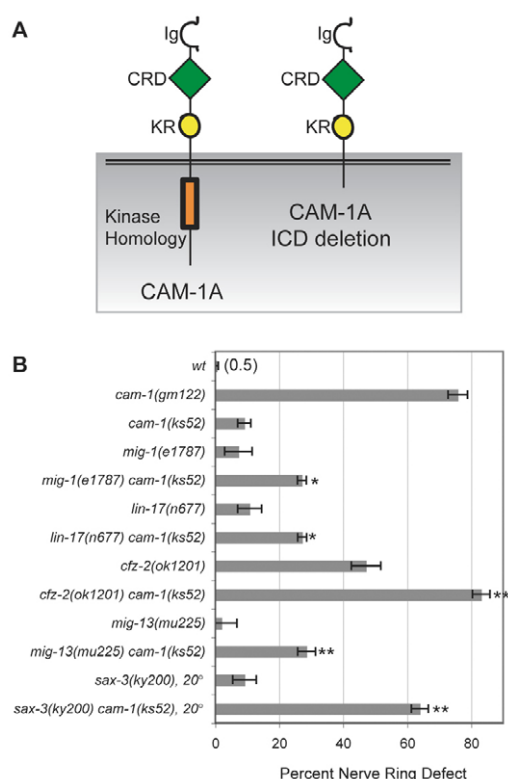


Fig. 5. Double mutants uncover a function for the intracellular domain of CAM-1. (A) Schematic of CAM-1 and the CAM-1(ks52) protein with a deleted intracellular domain (ICD). Ig, immunoglobulin domain; CRD, cysteine-rich domain; KR, Kring domain. (B) Nerve ring defects in *cam-1(ks52)* mutants and double mutants. Error bars represent the s.e. of proportion. Asterisks indicate double mutants different from either single mutant by Student's *t*-test or Fisher's exact test with Bonferroni correction. *, $P < 0.05$; **, $P < 0.01$.

observed with *cam-1A::cam-1A* and *cam-1B::cam-1B* transgenes, but not with *cam-1C::cam-1C* transgenes (Fig. 6B). *cam-1C::cam-1C* probably failed to rescue owing to its expression pattern, because a *cam-1A::cam-1C* transgene rescued *cam-1* (Fig. 6B). These results suggest that *cam-1A* and *cam-1B* upstream regions are expressed in cells that regulate nerve ring placement.

cam-1A and *cam-1B* upstream regions drive overlapping expression in neurons and head muscles (Koga et al., 1999), and pan-neuronal expression of *cam-1A* from the *unc-119* promoter rescued nerve ring placement, suggesting a neuronal site of action (Fig. 6B). Subsets of head neurons were tested using promoter fragments expressed around the comma stage of embryogenesis. Transgenes that were expressed in multiple sensory neurons and interneurons failed to rescue *cam-1* efficiently (*nsy-5::cam-1A*, *ncs-1::cam-1A*, *opt-3::cam-1A*), although these cells overlap with those that normally express *cam-1* (Fig. 6B). However, *cam-1A* expression in SIA, SIB and SMD motoneurons from the *ceh-24* promoter (Harfe and Fire, 1998) resulted in near-complete rescue of the *cam-1* nerve ring defect (Fig. 6B). A *mig-1::cam-1A* transgene also rescued *cam-1* mutants; this transgene overlaps with *ceh-24* in SIA and SIB, but not SMD, neurons (S. Clark and C.I.B., unpublished observations). A *cwn-2::cam-1A* transgene failed to rescue *cam-1* mutants; this transgene overlaps with *ceh-24* in SMD neurons and is also expressed in muscles (Fig. 6B). These experiments suggest that a specific spatial expression pattern that includes SIA and SIB neurons is required for *cam-1* rescue.

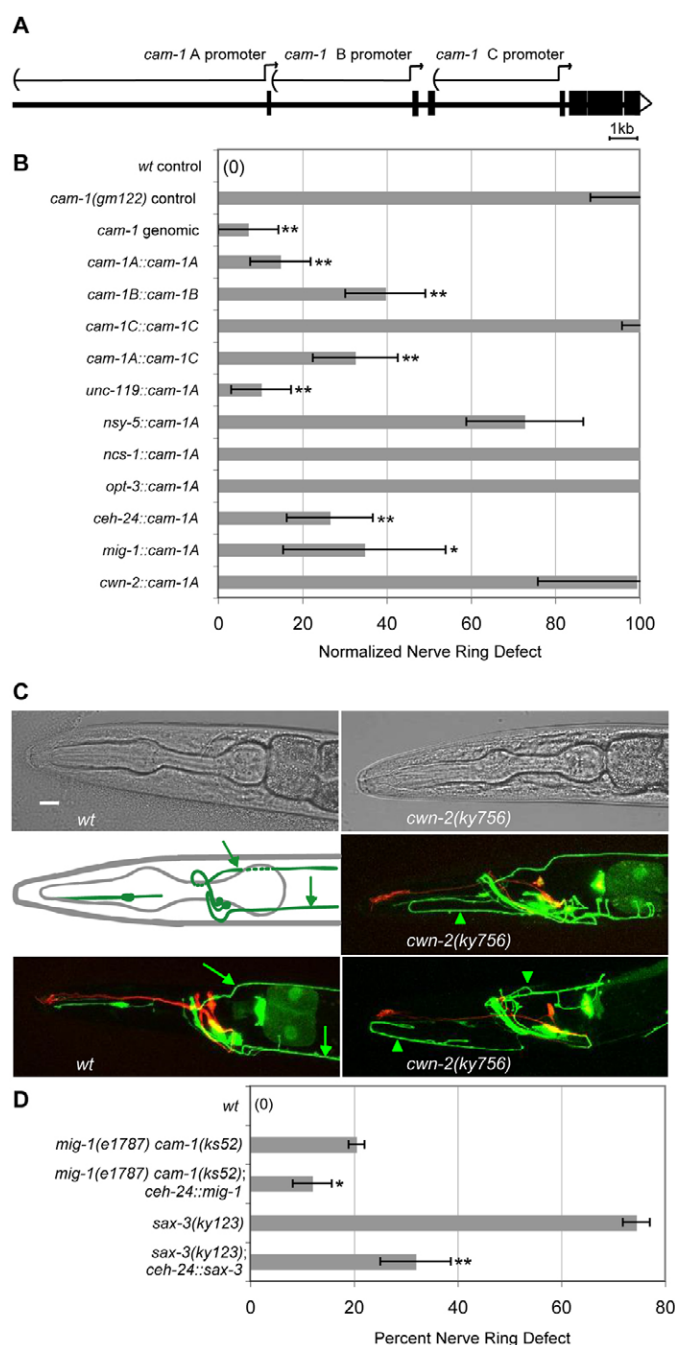


Fig. 6. *cam-1* functions in the SIA and/or SIB neurons to influence nerve ring placement. (A) Structure of the *cam-1* locus, showing *cam-1A*, *cam-1B* and *cam-1C* transcriptional start sites. (B) Transgenic rescue of *cam-1* nerve ring defects, scored at L4 stage. Defects in each strain were normalized to control siblings without the transgene (see Materials and methods). (C) Diagram and confocal projections of SIA, SIB and SMD neurons in wild type and *cwn-2* mutants. SIA, SIB and SMD neurons express *ceh-24::GFP* (green), as does a neuron within the pharynx. AWC and AWB neurons (red) mark the position of the nerve ring. Diagram shows the trajectories of two SIA neurons; SIB and SMD trajectories are comparable. Green arrows, dorsal and ventral sublateral cords; green arrowheads, aberrant axons. Anterior is left, dorsal is up. (D) Partial rescue of *mig-1* and *sax-3* nerve ring defects by cDNA expression in SIA, SIB and SMD neurons. In B and D, error bars represent the s.e. of proportion. Asterisks indicate values different from controls by Student's *t*-test or Fisher's exact test. *, $P < 0.05$; **, $P < 0.01$.

Each of the four SIA and four SIB neurons extends an axon anteriorly into the nerve ring, which then exits posteriorly in the ventral or dorsal sublateral nerve cord (Fig. 6C, green arrows). These neurons were examined in *cwn-2* mutants using a *ceh-24::GFP* transgene that labels all SIAs and SIBs, as well as two SMDs with similar morphologies. As with other nerve ring axons, *ceh-24::GFP*-expressing axons were shifted to an anterior position in *cwn-2* mutants. Unlike other nerve ring axons examined with *ceh-23::GFP* (sensory neurons) or *nmr-1::GFP* (interneurons), the *ceh-24*-expressing neurons had guidance errors at multiple positions. In many *cwn-2* animals, *ceh-24::GFP*-expressing axons made abnormal excursions anterior of the nerve ring (Fig. 6C, arrowheads). The *ceh-24::GFP* axons often failed to exit the nerve ring, or exited in the wrong place, failing to join the sublateral nerve cords. The defects in SIA and SIB were verified by electron microscopy, which showed that the *cwn-2* mutant animal had a reduced number of axons in the sublateral nerve cords (see Fig. S4 in the supplementary material). Despite this disorganization, several SIA and SIB markers (*ceh-24*, *cam-1* and *mig-1*) were expressed normally in *cwn-2* mutants.

cam-1 mutants had similar SIA and SIB defects to *cwn-2* mutants, whereas *cfz-2* mutants had milder defects and *mig-1* mutants appeared normal (see Table S5 in the supplementary material). Thus, the *ceh-24::GFP*-expressing neurons that are important for *cam-1* rescue are affected by *cwn-2* and *cam-1* mutations in more complex ways than other neurons in the nerve ring.

We next asked whether other candidate receptors affecting nerve ring placement might act in the SIA and SIB neurons. Expression of *mig-1* cDNA under the *ceh-24* promoter partially rescued the nerve ring defect in *mig-1 cam-1(ks52)* animals (Fig. 6D), and, similarly, a *ceh-24::sax-3* transgene partially rescued the *sax-3* nerve ring defect (Fig. 6D). A *ceh-24::cfz-2* transgene did not rescue a *cfz-2* mutant (see Table S3 in the supplementary material). These results suggest that *mig-1* (Frizzled) and *sax-3* (Robo) can act in the SIA, SIB or SMD neurons, and are in agreement with other genetic results suggesting that *cfz-2* can function independently of *cam-1*.

To further characterize the role of the SIA and SIB neurons in nerve ring development, we killed them by expressing the *egl-1* BH3 cell death gene in SIA, SIB and SMD neurons under the *ceh-24* promoter. The resulting transgene killed SIA, SIB and SMD neurons inefficiently, sparing a subset of neurons in most animals (see Materials and methods). Despite this inefficiency, 20% of animals with the transgene had a nerve ring placement defect resembling that of *cwn-2* mutants (Fig. 7). These results demonstrate that *ceh-24*-expressing neurons affect placement of the developing nerve ring. The anterior nerve ring defect of a *cwn-2* mutant was neither enhanced nor suppressed by the *ceh-24::egl-1* transgene (Fig. 7B). Using the logic of genetic interactions, this observation suggests that the *cwn-2* mutation and the *ceh-24::egl-1* transgene act in a common process to affect nerve ring development.

DISCUSSION

CWN-2 has an essential role in nerve ring placement (Fig. 8A). Our results suggest that CWN-2 is a ligand for the CAM-1 (Ror) receptor in the SIA and SIB neurons, perhaps with MIG-1 (Frizzled) as a co-receptor. In the absence of this signaling pathway, many axons and cell bodies in the nerve ring are displaced towards the anterior. The similar effects of Wnt pathway mutations and genetic ablations suggest that SIA and SIB neurons direct normal nerve ring placement. Additional nerve ring guidance genes that act at least partly parallel to *cwn-2*, *cam-1* and *mig-1* are the Frizzled gene *cfz-2*, the Wnt gene *cwn-1*, and the Robo gene *sax-3*.

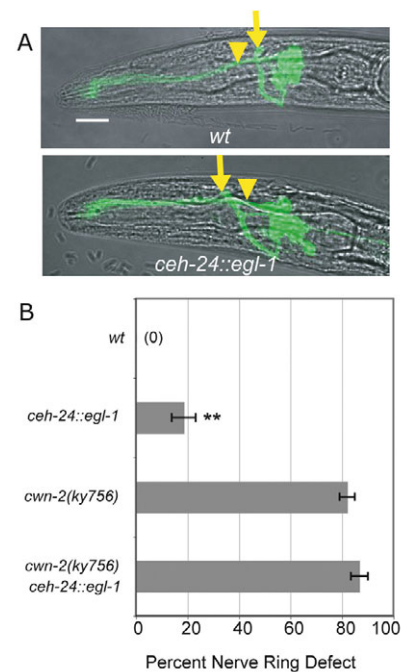


Fig. 7. Nerve ring defects caused by ablation of SIA, SIB and SMD neurons. (A) *C. elegans* L1 larvae illustrating anterior nerve rings in animals carrying a *ceh-24::egl-1* transgene. Images are confocal projections of *ceh-23::GFP* merged with a bright-field image. Arrows, nerve ring position; arrowheads, the posterior boundary of the metacarpus (as in Fig. 1). Anterior is left, dorsal is up. Scale bar: 10 μ m. (B) Quantification of nerve ring defects in animals carrying *ceh-24::egl-1* transgene in control and *cwn-2* mutant backgrounds. All animals were *ced-3/+* heterozygotes. Error bars represent the s.e. of proportion. Asterisks indicate values different from controls by Student's *t*-test or Fisher's exact test. **, $P < 0.01$.

cwn-2 is required at a discrete time in development, but the site of *cwn-2* expression is relatively unimportant. The rescue of *cwn-2* mutants by uniform expression or misexpression echoes the rescue of *egl-20* and *lin-44* Wnt defects by cDNAs expressed from heat-shock promoters (Hilliard and Bargmann, 2006; Whangbo and Kenyon, 1999), and suggests that *C. elegans* Wnts can sometimes function as non-spatial cues. For example, CWN-2 could stimulate axon outgrowth of SIA and SIB at a particular time, with spatial information provided by the distribution of receptors or by other guidance cues near the nerve ring, such as UNC-6 and SLT-1. Alternatively, *cwn-2* activity could be spatially limited by cell-specific post-translational pathways (Coudreuse and Korswagen, 2007; Pan et al., 2008; Yang et al., 2008) or by extracellular Wnt-binding proteins (Dierick and Bejsovec, 1998; Green et al., 2007). Finally, additional Wnts, such as CWN-1, might contribute spatial information when CWN-2 is misexpressed: disrupting *cwn-2* alone may not eliminate the overall posteriorly biased pattern of Wnt expression (Fig. 8A). Indeed, in the posterior body, overlapping functions of *lin-44*, *egl-20* and *cwn-1* can mask the effects of misexpressing a single Wnt (Klassen and Shen, 2007).

CAM-1 has been proposed to act as an extracellular inhibitor of Wnts owing to its non-cell-autonomous action in vulval development and the apparent dispensability of its intracellular domain (Forrester et al., 2004; Green et al., 2007). However, the CAM-1-related protein Ror2 is an established tyrosine kinase receptor for mammalian Wnts (Mikels and Nusse, 2006), although

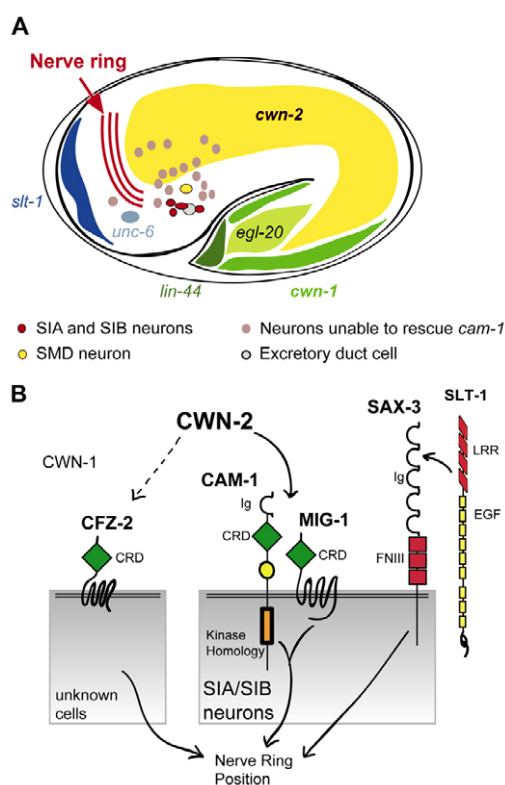


Fig. 8. Cellular and molecular models for nerve ring placement.

(A) Diagram of a *C. elegans* embryo near the time of nerve ring formation, showing cells and cues relevant for nerve ring guidance (this work) (Wadsworth et al., 1996; Hao et al., 2001; Pan et al., 2006; Whangbo and Kenyon, 1999). Gray neurons, which are negative for *cam-1* rescue based on Fig. 6B, include BAG, ASK, ADL, ASI, AWC, ASH, AFD, ADF, AWB, AVE, AIM, AIY, AVK, AIZ, RIC, ADA, RMG, PHA, PHV, PVC and PVQ. (B) CAM-1 may be a receptor for CWN-2 in SIA and/or SIB neurons. MIG-1 (Frizzled) may be a co-receptor for CWN-2 in SIA and SIB. The SLT-1 receptor SAX-3 also affects nerve ring development, and can function in the same cells. CFZ-2 affects nerve ring development at an unknown site, and CWN-1 has mild effects on nerve ring development. Ig, immunoglobulin domain; CRD, cysteine-rich domain; KR, Kringle domain; FNIII, Fibronectin type III domain; LRR, leucine-rich repeat; EGF, Epidermal growth factor repeat.

kinase-independent functions are also known for vertebrate Rors (Hikasa et al., 2002). Nerve ring development initially appeared not to require the intracellular domain of CAM-1, but many double mutants that included the Frizzleds *mig-1*, *cfz-2* and *lin-17* and the LRP-like *mig-13* uncovered a requirement for the intracellular domain. Together with a specific requirement for *cam-1* expression in the SIA and SIB neurons, these results support a receptor function of CAM-1 in nerve ring development. The overlapping expression and rescue of *cam-1* and *mig-1* in SIA and SIB matches the genetic results suggesting that they act together in a common process, perhaps as co-receptors for CWN-2 (Fig. 8B). In mammalian osteocytes and lung epithelial cells, Frizzled and Ror or Ryk receptors can function together in a signaling complex (Billiard et al., 2005; Li et al., 2008). The relevant cellular sites of action for *cfz-2*, *lin-17* and *mig-13* are unknown, and expression of *cfz-2* in SIA and SIB neurons did not rescue *cfz-2* mutants, suggesting that *cfz-2* has primary functions outside of SIA and SIB. It is too early to determine whether CFZ-2, LIN-17 and MIG-13 might also be CAM-1 co-receptors.

One interesting implication of the use of multiple Wnt receptors is that spatially and temporally restricted receptor expression might be as important in development as restricted ligand expression. Rather than responding passively to an instructive Wnt cue, developing neurons can shape their response to Wnts through their receptor complement. They can also shape the response of more-distant cells by capturing Wnt ligands, as shown for CAM-1 near the vulva (Green et al., 2007).

Cell-type-specific rescue of *cam-1*, *mig-1* and *sax-3* and cell ablation experiments revealed an important role for SIA and SIB neurons in nerve ring placement. Several models could explain *cwn-2* effects on SIA and SIB. First, *cwn-2* could act in a traditional Wnt patterning role to determine SIA and SIB cell fates; SIA and SIB would then organize nerve ring development through other molecular pathways. However, several SIA and SIB markers are expressed normally in *cwn-2* mutants, arguing against a cell fate change.

We favor the model that *cwn-2* directly affects axon guidance of SIA and SIB neurons, which in turn instruct the positioning of the nerve ring. SIA and SIB neurons occupy a position near the base of the nerve ring, where they might detect CWN-2, as well as the ventral attractant UNC-6 and the anterior repellent SLT-1 (Fig. 8A). In wild-type animals, the nerve ring axon trajectories of SIA and SIB neurons are unusually complex, consistent with a special patterning role (Fig. 6C). In *cwn-2* and *cam-1* mutants, the disruption of axon trajectories in SIA and SIB neurons is more complicated than in other cell types: SIA and SIB have guidance defects at many positions, whereas other neurons simply move to an anterior location. We suggest that the guidance of SIA and SIB neurons is under the direct control of CWN-2, which generates a temporally precise and spatially less precise signal to form a nerve ring at the correct location. Other nerve ring neurons follow SIA and SIB neurons to this location if possible; if SIA and SIB neurons are misguided or absent, the nerve ring shifts to a more anterior position that might be a default position, or one specified by another guidance cue.

Acknowledgements

We thank Michael Francis, Massimo Hilliard, Tinya Fleming, Gian Garriga, the *C. elegans* Gene Knockout Consortium, the Sanger Institute and Yuji Kohara for strains and reagents; and Massimo Hilliard, Tapan Maniar, Jennifer Garrison, Sreekanth Chalasani and Yasunori Saheki for comments on the manuscript. This work was supported by HHMI. J.R.K. was supported by an HHMI Predoctoral Fellowship and C.I.B. is an Investigator of HHMI. Deposited in PMC for release after 6 months.

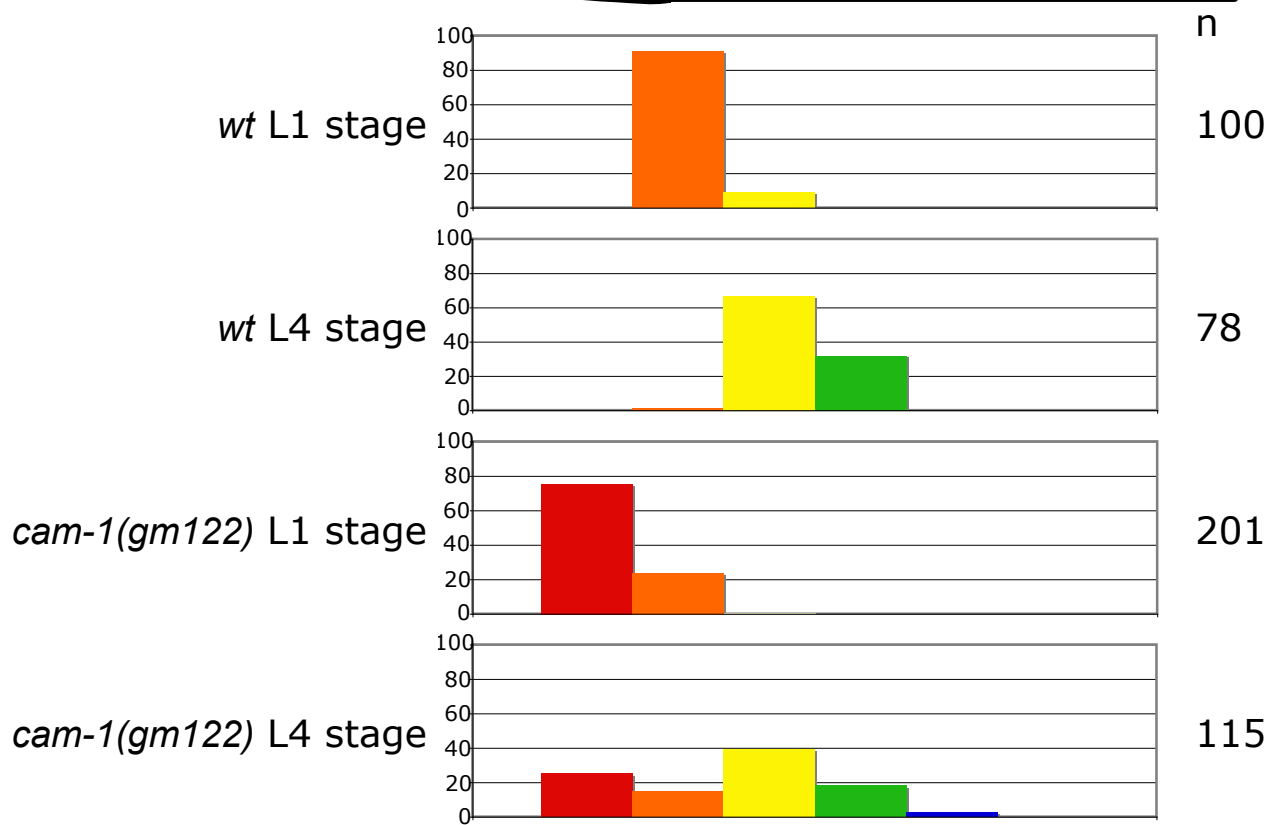
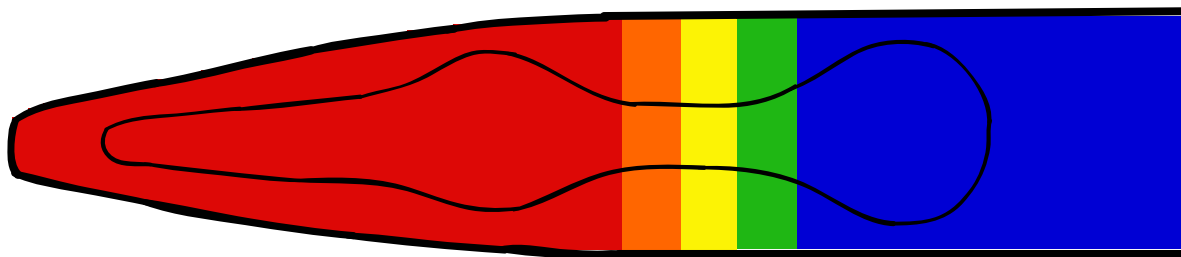
Supplementary material

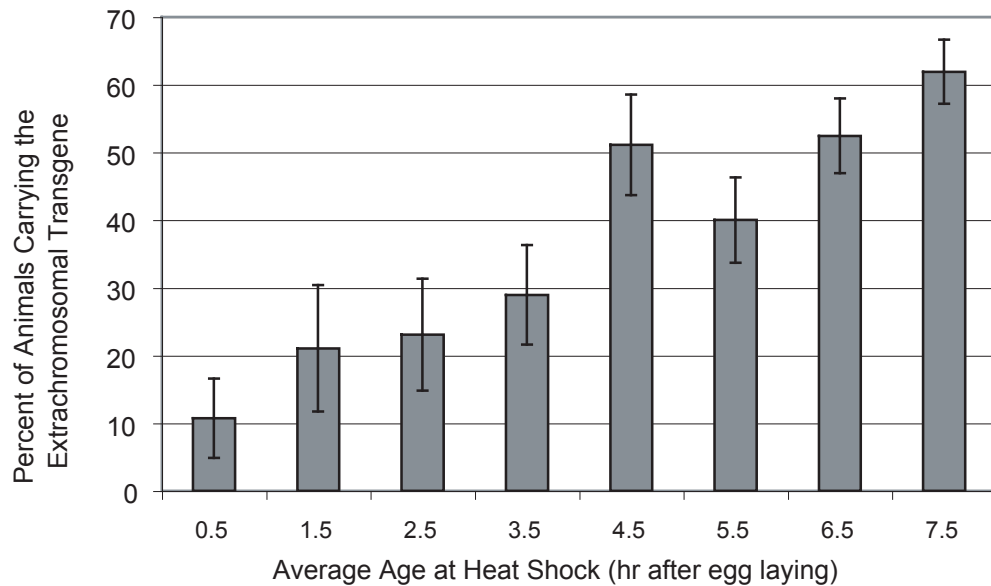
Supplementary material for this article is available at <http://dev.biologists.org/cgi/content/full/136/22/3801/DC1>

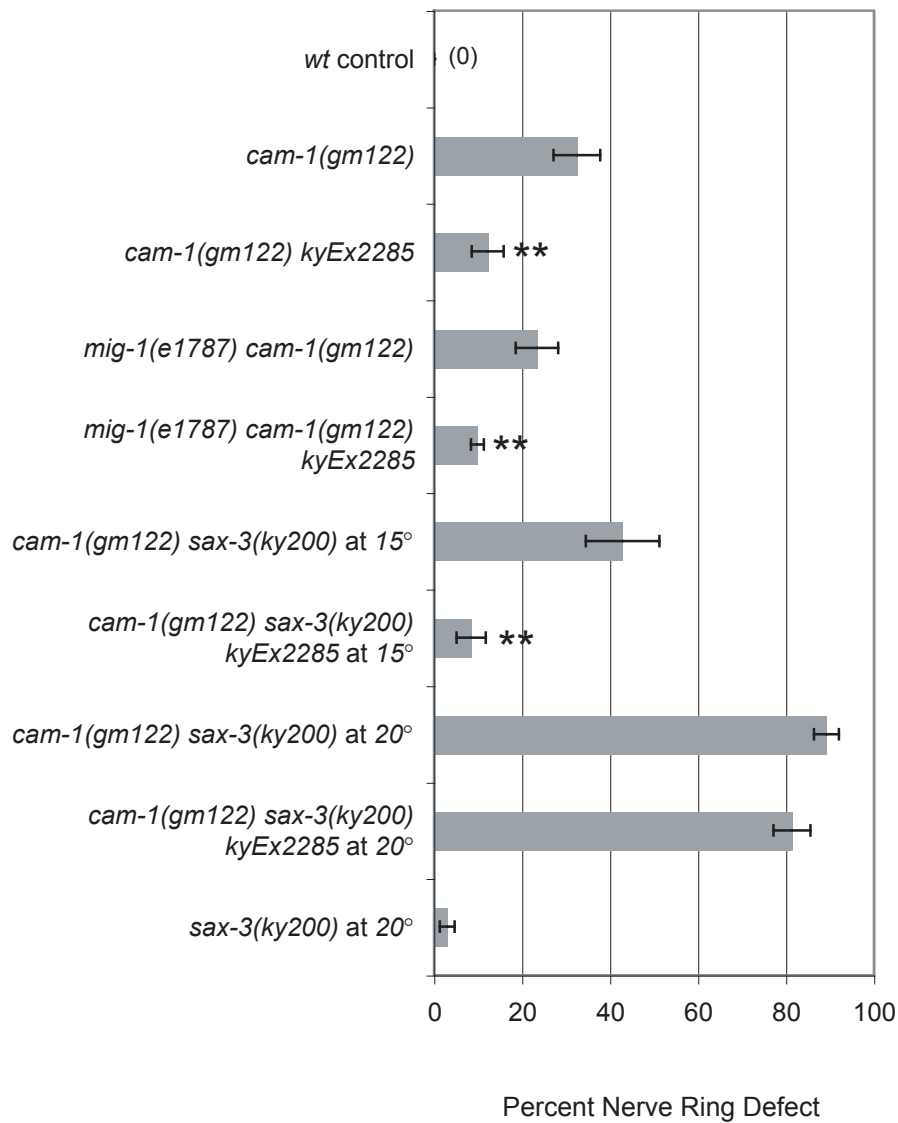
References

- Adler, C. E., Fetter, R. D. and Bargmann, C. I. (2006). UNC-6/Netrin induces neuronal asymmetry and defines the site of axon formation. *Nat. Neurosci.* **9**, 511–518.
- Aurelio, O., Hall, D. H. and Hobert, O. (2002). Immunoglobulin-domain proteins required for maintenance of ventral nerve cord organization. *Science* **295**, 686–690.
- Benard, C. Y., Boyanov, A., Hall, D. H. and Hobert, O. (2006). DIG-1, a novel giant protein, non-autonomously mediates maintenance of nervous system architecture. *Development* **133**, 3329–3340.
- Billiard, J., Way, D. S., Seestaller-Wehr, L. M., Moran, R. A., Mangine, A. and Bodine, P. V. (2005). The orphan receptor tyrosine kinase Ror2 modulates canonical Wnt signaling in osteoblastic cells. *Mol. Endocrinol.* **19**, 90–101.
- Brenner, S. (1974). The genetics of *Caenorhabditis elegans*. *Genetics* **77**, 71–94.
- Coates, J. C. and de Bono, M. (2002). Antagonistic pathways in neurons exposed to body fluid regulate social feeding in *Caenorhabditis elegans*. *Nature* **419**, 925–929.
- Colón-Ramos, D. A., Margeta, M. A. and Shen, K. (2007). Glia promote local synaptogenesis through UNC-6 (netrin) signaling in *C. elegans*. *Science* **318**, 103–106.

- Coudreuse, D. and Korswagen, H. C. (2007). The making of Wnt: new insights into Wnt maturation, sorting and secretion. *Development* **134**, 3-12.
- Dierick, H. A. and Bejsovec, A. (1998). Functional analysis of Wingless reveals a link between intercellular ligand transport and dorsal-cell-specific signaling. *Development* **125**, 4729-4738.
- Epstein, H. F., Shakes, D. C. and American Society for Cell Biology (1995). *Caenorhabditis elegans: Modern Biological Analysis of an Organism*. San Diego: Academic Press.
- Forrester, W. C., Dell, M., Perens, E. and Garriga, G. (1999). A C. elegans Ror receptor tyrosine kinase regulates cell motility and asymmetric cell division. *Nature* **400**, 881-885.
- Forrester, W. C., Kim, C. and Garriga, G. (2004). The Caenorhabditis elegans Ror RTK CAM-1 inhibits EGL-20/Wnt signaling in cell migration. *Genetics* **168**, 1951-1962.
- Fradkin, L. G., Garriga, G., Salinas, P. C., Thomas, J. B., Yu, X. and Zou, Y. (2005). Wnt signaling in neural circuit development. *J. Neurosci.* **25**, 10376-10378.
- Francis, M. M., Evans, S. P., Jensen, M., Madsen, D. M., Mancuso, J., Norman, K. R. and Maricq, A. V. (2005). The Ror receptor tyrosine kinase CAM-1 is required for ACR-16-mediated synaptic transmission at the C. elegans neuromuscular junction. *Neuron* **46**, 581-594.
- Gleason, J. E., Szyleyko, E. A. and Eisenmann, D. M. (2006). Multiple redundant Wnt signaling components function in two processes during C. elegans vulval development. *Dev. Biol.* **298**, 442-457.
- Goldstein, B., Takeshita, H., Mizumoto, K. and Sawa, H. (2006). Wnt signals can function as positional cues in establishing cell polarity. *Dev. Cell* **10**, 391-396.
- Green, J. L., Inoue, T. and Sternberg, P. W. (2007). The C. elegans ROR receptor tyrosine kinase, CAM-1, non-autonomously inhibits the Wnt pathway. *Development* **134**, 4053-4062.
- Green, J. L., Inoue, T. and Sternberg, P. W. (2008a). Opposing Wnt pathways orient cell polarity during organogenesis. *Cell* **134**, 646-656.
- Green, J. L., Kuntz, S. G. and Sternberg, P. W. (2008b). Ror receptor tyrosine kinases: orphans no more. *Trends Cell Biol.* **18**, 536-544.
- Guarente, L. (1993). Synthetic enhancement in gene interaction: a genetic tool come of age. *Trends Genet.* **9**, 362-366.
- Hao, J. C., Yu, T. W., Fujisawa, K., Culotti, J. G., Gengyo-Ando, K., Mitani, S., Moulder, G., Barstead, R., Tessier-Lavigne, M. and Bargmann, C. I. (2001). C. elegans slit acts in midline, dorsal-ventral, and anterior-posterior guidance via the SAX-3/Robo receptor. *Neuron* **32**, 25-38.
- Harfe, B. D. and Fire, A. (1998). Muscle and nerve-specific regulation of a novel NK-2 class homeodomain factor in Caenorhabditis elegans. *Development* **125**, 421-429.
- Herman, M. A., Vassilieva, L. L., Horvitz, H. R., Shaw, J. E. and Herman, R. K. (1995). The C. elegans gene lin-44, which controls the polarity of certain asymmetric cell divisions, encodes a Wnt protein and acts cell nonautonomously. *Cell* **83**, 101-110.
- Hikasa, H., Shibata, M., Hiratani, I. and Taira, M. (2002). The Xenopus receptor tyrosine kinase Xr2 modulates morphogenetic movements of the axial mesoderm and neuroectoderm via Wnt signaling. *Development* **129**, 5227-5239.
- Hilliard, M. A. and Bargmann, C. I. (2006). Wnt signals and frizzled activity orient anterior-posterior axon outgrowth in C. elegans. *Dev. Cell* **10**, 379-390.
- Keeble, T. R., Halford, M. M., Seaman, C., Kee, N., Macheda, M., Anderson, R. B., Stacker, S. A. and Cooper, H. M. (2006). The Wnt receptor Ryk is required for Wnt5a-mediated axon guidance on the contralateral side of the corpus callosum. *J. Neurosci.* **26**, 5840-5848.
- Kim, C. and Forrester, W. C. (2003). Functional analysis of the domains of the C. elegans Ror receptor tyrosine kinase CAM-1. *Dev. Biol.* **264**, 376-390.
- Klassen, M. P. and Shen, K. (2007). Wnt signaling positions neuromuscular connectivity by inhibiting synapse formation in C. elegans. *Cell* **130**, 704-716.
- Koga, M., Takeuchi, M., Tameishi, T. and Ohshima, Y. (1999). Control of DAF-7 TGF- α expression and neuronal process development by a receptor tyrosine kinase KIN-8 in Caenorhabditis elegans. *Development* **126**, 5387-5398.
- Kremer, J. R., Mastrorade, D. N. and McIntosh, J. R. (1996). Computer visualization of three-dimensional image data using IMOD. *J. Struct. Biol.* **116**, 71-76.
- Li, C., Chen, H., Hu, L., Xing, Y., Sasaki, T., Villosis, M. F., Li, J., Nishita, M., Minami, Y. and Minoo, P. (2008). Ror2 modulates the canonical Wnt signaling in lung epithelial cells through cooperation with Fzd2. *BMC Mol. Biol.* **9**, 11.
- Liu, Y., Rubin, B., Bodine, P. V. and Billiard, J. (2008). Wnt5a induces homodimerization and activation of Ror2 receptor tyrosine kinase. *J. Cell. Biochem.* **105**, 497-502.
- Logan, C. Y. and Nusse, R. (2004). The Wnt signaling pathway in development and disease. *Annu. Rev. Cell Dev. Biol.* **20**, 781-810.
- Lu, W., Yamamoto, V., Ortega, B. and Baltimore, D. (2004). Mammalian Ryk is a Wnt coreceptor required for stimulation of neurite outgrowth. *Cell* **119**, 97-108.
- Lyuksytova, A. I., Lu, C. C., Milanesio, N., King, L. A., Guo, N., Wang, Y., Nathans, J., Tessier-Lavigne, M. and Zou, Y. (2003). Anterior-posterior guidance of commissural axons by Wnt-frizzled signaling. *Science* **302**, 1984-1988.
- Mikels, A. J. and Nusse, R. (2006). Purified Wnt5a protein activates or inhibits beta-catenin-TCF signaling depending on receptor context. *PLoS Biol.* **4**, e115.
- Pan, C. L., Howell, J. E., Clark, S. G., Hilliard, M., Cordes, S., Bargmann, C. I. and Garriga, G. (2006). Multiple Wnts and frizzled receptors regulate anteriorly directed cell and growth cone migrations in Caenorhabditis elegans. *Dev. Cell* **10**, 367-377.
- Pan, C. L., Baum, P. D., Gu, M., Jorgensen, E. M., Clark, S. G. and Garriga, G. (2008). C. elegans AP-2 and retromer control Wnt signaling by regulating mig-14/Wntless. *Dev. Cell* **14**, 132-139.
- Prasad, B. C. and Clark, S. G. (2006). Wnt signaling establishes anteroposterior neuronal polarity and requires retromer in C. elegans. *Development* **133**, 1757-1766.
- Rocheau, C. E., Downs, W. D., Lin, R., Wittmann, C., Bei, Y., Cha, Y. H., Ali, M., Priess, J. R. and Mello, C. C. (1997). Wnt signaling and an APC-related gene specify endoderm in early C. elegans embryos. *Cell* **90**, 707-716.
- Sasakura, H., Inada, H., Kuhara, A., Fusaoka, E., Takemoto, D., Takeuchi, K. and Mori, I. (2005). Maintenance of neuronal positions in organized ganglia by SAX-7, a Caenorhabditis elegans homologue of L1. *EMBO J.* **24**, 1477-1488.
- Suzuki, Y. and Han, M. (2006). Genetic redundancy masks diverse functions of the tumor suppressor gene PTEN during C. elegans development. *Genes Dev.* **20**, 423-428.
- Sym, M., Robinson, N. and Kenyon, C. (1999). MIG-13 positions migrating cells along the anteroposterior body axis of C. elegans. *Cell* **98**, 25-36.
- Tolwinski, N. S., Wehrli, M., Rives, A., Erdeniz, N., DiNardo, S. and Wieschaus, E. (2003). Wg/Wnt signal can be transmitted through arrow/LRP5,6 and Axin independently of Zw3/Gsk3 β activity. *Dev. Cell* **4**, 407-418.
- van Amerongen, R., Mikels, A. and Nusse, R. (2008). Alternative wnt signaling is initiated by distinct receptors. *Sci. Signal.* **1**, re9.
- Wadsworth, W. G., Bhatt, H. and Hedgecock, E. M. (1996). Neuroglia and pioneer neurons express UNC-6 to provide global and local netrin cues for guiding migrations in C. elegans. *Neuron* **16**, 35-46.
- Wehrli, M., Dougan, S. T., Caldwell, K., O'Keefe, L., Schwartz, S., Vaizel-Ohayon, D., Schejter, E., Tomlinson, A. and DiNardo, S. (2000). arrow encodes an LDL-receptor-related protein essential for Wingless signalling. *Nature* **407**, 527-530.
- Whangbo, J. and Kenyon, C. (1999). A Wnt signaling system that specifies two patterns of cell migration in C. elegans. *Mol. Cell* **4**, 851-858.
- White, J., Southgate, E., Thomson, J. N. and Brenner, S. (1986). The structure of the nervous system of the nematode Caenorhabditis elegans. *Philos. Trans. R. Soc. Lond. B* **314**, 1-340.
- Yamamoto, S., Nishimura, O., Misaki, K., Nishita, M., Minami, Y., Yonemura, S., Tarui, H. and Sasaki, H. (2008). Cthrc1 selectively activates the planar cell polarity pathway of Wnt signaling by stabilizing the Wnt-receptor complex. *Dev. Cell* **15**, 23-36.
- Yang, P. T., Lorenowicz, M. J., Silhankova, M., Coudreuse, D. Y., Betist, M. C. and Korswagen, H. C. (2008). Wnt signaling requires retromer-dependent recycling of MIG-14/Wntless in Wnt-producing cells. *Dev. Cell* **14**, 140-147.
- Yoshikawa, S., McKinnon, R. D., Kokel, M. and Thomas, J. B. (2003). Wnt-mediated axon guidance via the Drosophila Derailed receptor. *Nature* **422**, 583-588.
- Yoshimura, S., Murray, J. I., Lu, Y., Waterston, R. H. and Shaham, S. (2008). mls-2 and vab-3 Control glia development, hlh-17/Olig expression and glia-dependent neurite extension in C. elegans. *Development* **135**, 2263-2275.
- Zallen, J. A., Yi, B. A. and Bargmann, C. I. (1998). The conserved immunoglobulin superfamily member SAX-3/Robo directs multiple aspects of axon guidance in C. elegans. *Cell* **92**, 217-227.
- Zallen, J. A., Kirch, S. A. and Bargmann, C. I. (1999). Genes required for axon pathfinding and extension in the C. elegans nerve ring. *Development* **126**, 3679-3692.
- Zinovyeva, A. Y. and Forrester, W. C. (2005). The C. elegans Frizzled CFZ-2 is required for cell migration and interacts with multiple Wnt signaling pathways. *Dev. Biol.* **285**, 447-461.
- Zinovyeva, A. Y., Yamamoto, Y., Sawa, H. and Forrester, W. C. (2008). Complex network of Wnt signaling regulates neuronal migrations during Caenorhabditis elegans development. *Genetics* **179**, 1357-1371.







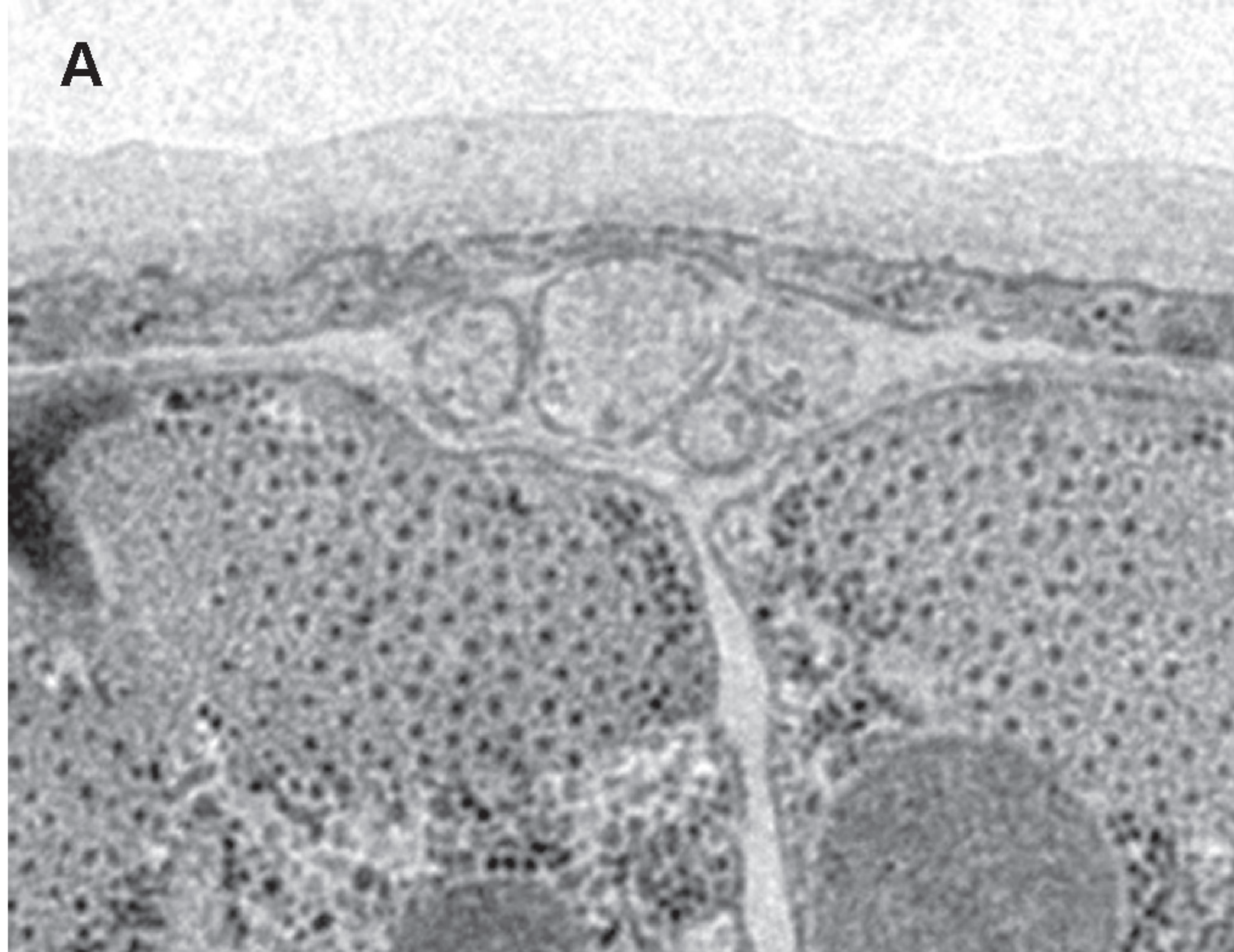
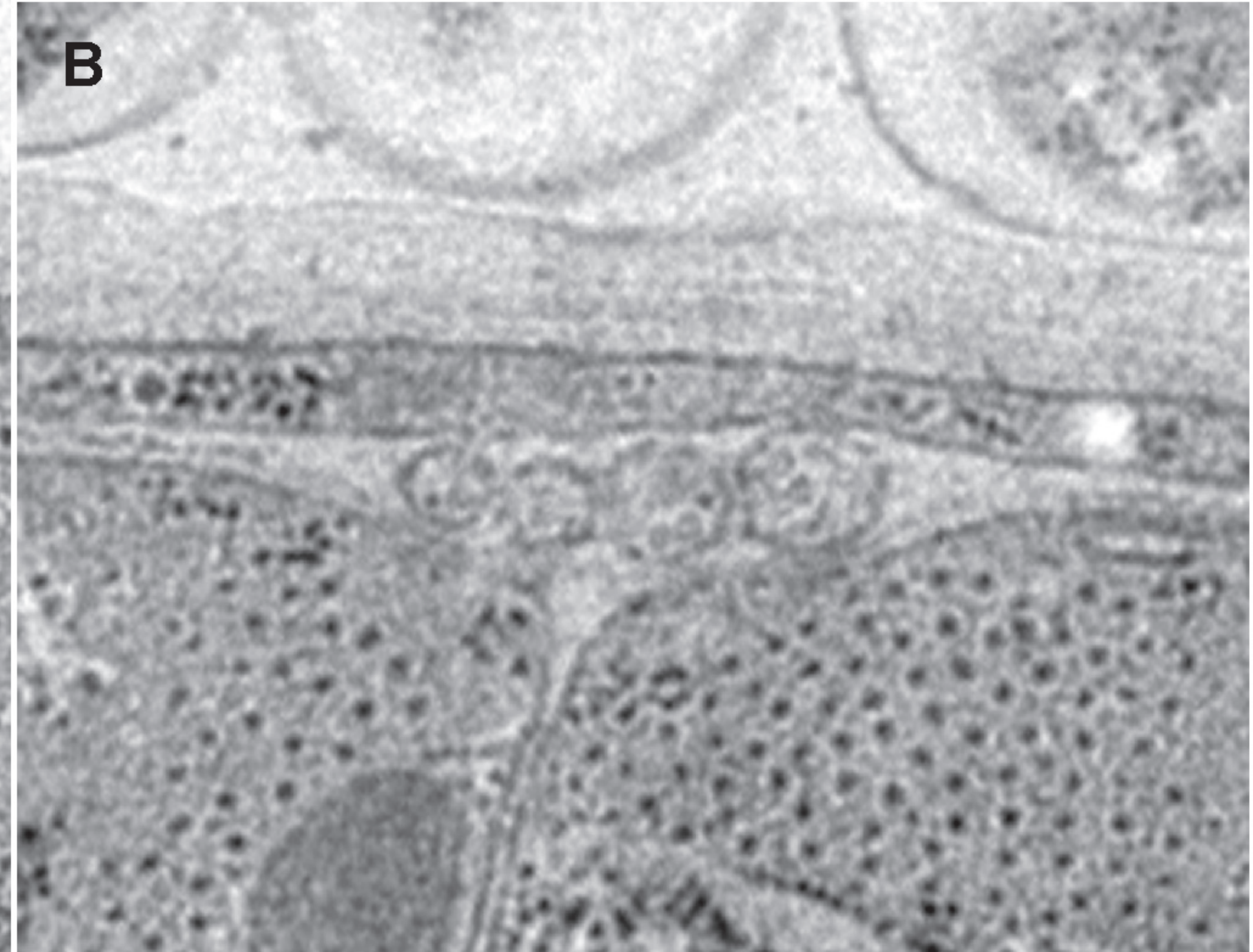
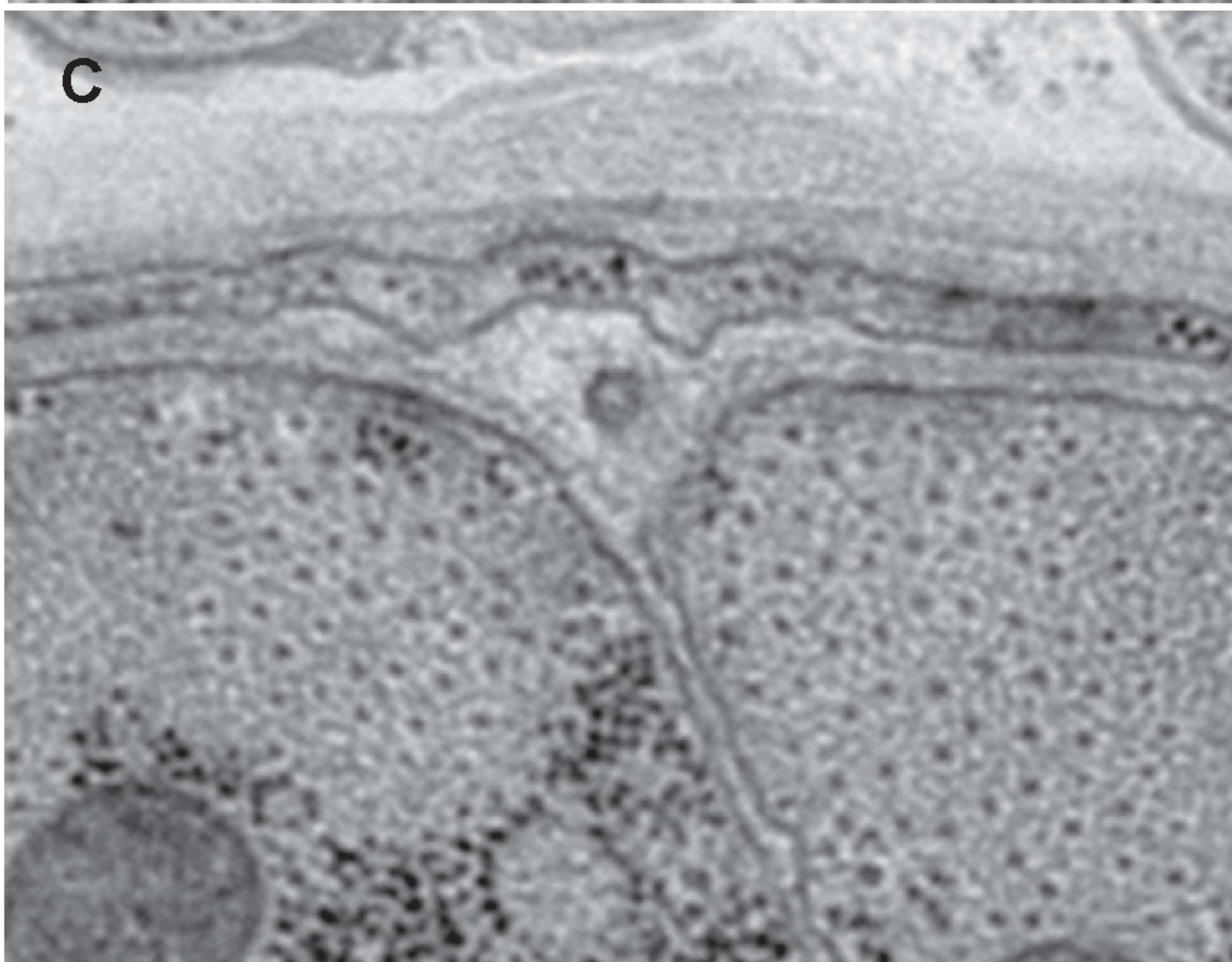
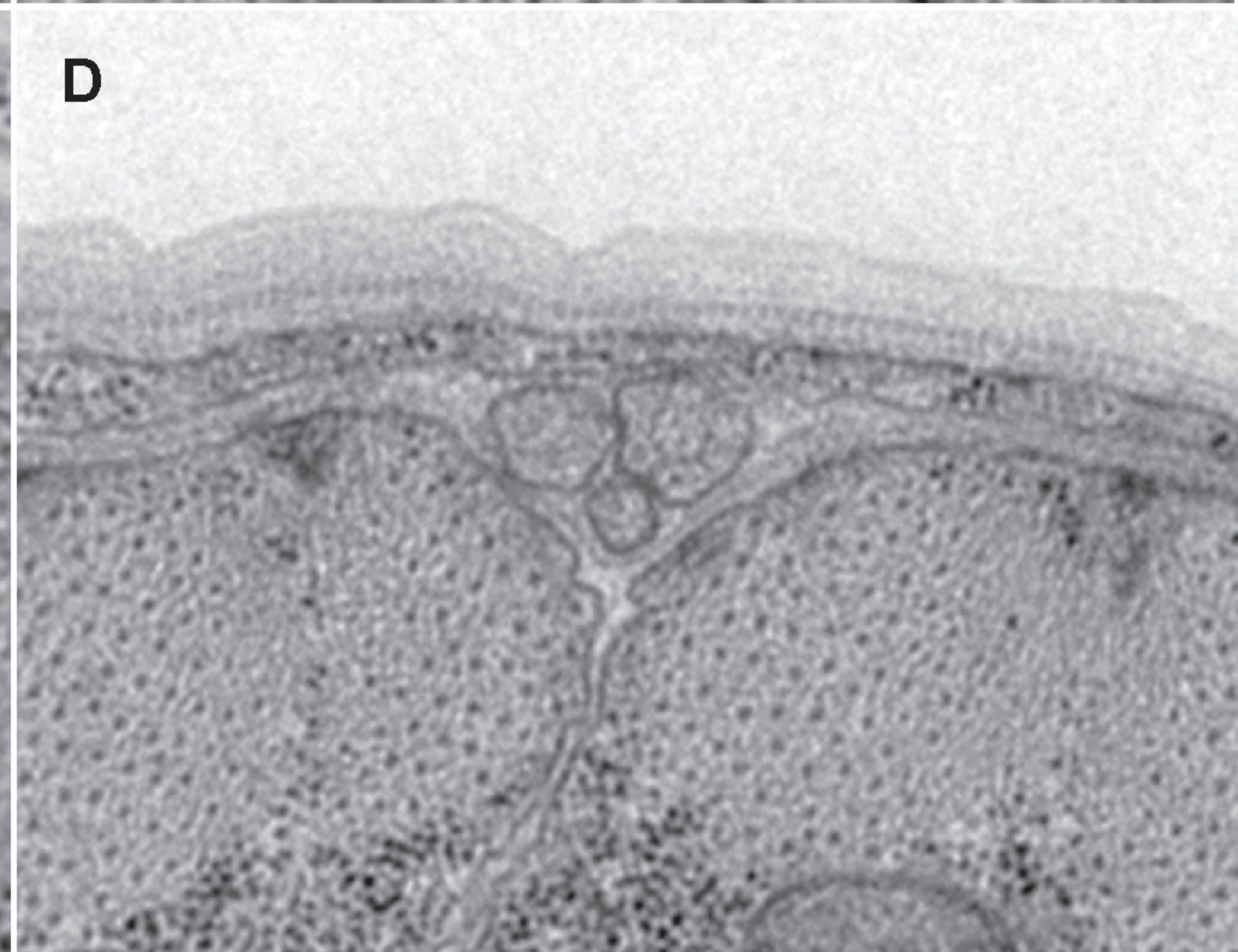
A*wt***B****C***cwn-2***D**

Table S1. Genotyping primers

Gene (allele)	Primers (5' to 3')	Polymorphism	Wild type	Mutant
<i>slt-1(eh15)</i>	CCCCGCTTTGCAACACAACCTC CTGCACACCGTTGCTTATCT	<i>DdeI</i>	273, 184, 151	279, 273, 184, 53
<i>sax-3(ky200)</i>	ATCGGTGAGGGAAGGTGTTTCGTTT AGATGGCTTTGCACCACAGTTGAG	<i>FokI</i>	346	283, 63
<i>cwn-2(ky736)</i>	TCGCCTGGTCAAGCTCAAGTATGT CGAAGGAAGTTGCATCCAACAGGT	<i>HphI</i>	500, 137	637
<i>cwn-2(ky756)</i>	GAAGACGGTGCAAACAGGGACTTT GGCAACATACTTGCAAACCTTCC	Sequence		
<i>cwn-2(ok895)</i>	GAAGACGGTGCAAACAGGGACTTT ATCCGTTGGCAATGCTCTTGT	PCR length	545	No product
	TGTGAGCTTTTCAAAGATCATATGCC TGGGGTGAACGAAACCCATAAG	PCR length	1268	363
<i>cam-1(gm122)</i>	TGTCGCTGTATCAGAACGATGGCT GTGCCAATTCTGATGGGCATTCTGT	<i>MseI</i>	397	274, 123
<i>cam-1(ks52)</i>	AGTAGCTCTTGTTGGTGGTGGAGT TATCCACGTTGATGGGTTGGTGGT	PCR length	1389	325
	TCACGAGTTGCTGAAGGTTTCGAGT TGTTGGTTGGACAATTGTGAGGGC	PCR length	512	No product
<i>cfz-2(ok1201)</i>	AAATATGCATTTCTTGAGCACTACAGC AAGAAGCCGGATTGGAAGTT	PCR length	2899	1725
	GATAACTGGAATCTGCTACGTGGG GCACAACTGCGATTGCTCCCATAA	PCR length	307	No product
<i>lin-17(n677)</i>	TTCTACCTATCCCTGTGCATCT CTAATTCTCTCTGCACATGCTC	<i>BanI</i>	287, 251	538
<i>mig-1(e1787)</i>	CGTTTGAAAGTTGGCGGCCTAGAAT TGTCCCTGTGCGCCTTATTCCACGA	Sequence		
<i>cwn-1(ok546)</i>	AATCACTGAAAGGGCTCACCAGGA ACTCTCCGTTGAGCGGAATCAACA	PCR length	1145	360
	TCCTCTAGCACAACTCTCGGGTAAC TGCTTATGCAGATAGACCACACGG	PCR length	492	No product
<i>lin-44(n1792)</i>	ATTACTTAAAGGCGCATACTGC ATCGTCAATCCATCCTTGTG	<i>BsrDI</i>	240, 187	427
<i>egl-20(n585)</i>	TCCATCTGCCACATACGTACGCA CCGTGACGAGTTTCTGTAACTT	Sequence		
<i>mig-13(mu225)</i>	TATTAGTCAACCACCACCACCGCA TGCATAGCTTTCCGGATCGAGTGT	Sequence		
<i>ced-3(n717)</i>	TTGAAAGTGGGCGGAGTGAATTGC GACTTCAGTCAGCAGCTCAACAAC	Sequence		

Table S2. Strain list

Strain	Genotype	Plasmid	Reference
CX7465	<i>cwn-2(ok895) IV; lin-15(n765) X; kyEx902[cwn-2 genomic::SL2::GFP, lin-15(+)]</i>	pJRK20	
CX8072	<i>lin-15(n765) X; kyEx902[cwn-2 genomic::SL2::GFP, lin-15(+)]</i>	pJRK20	
CX8504	<i>cwn-2(ok895) IV; kyEx1464[elt-2::cwn-2, 100ng/uL, odr-1::RFP 50ng/uL]</i>	pJRK27	
CX8392	<i>cwn-2(ok895) IV; kyEx1380[myo-2::cwn-2, 100ng/uL, odr-1::RFP 50ng/uL]</i>	pJRK22	
CX8391	<i>cwn-2(ok895) IV; kyEx1379[slt-1::cwn-2, 100ng/uL, odr-1::RFP 50ng/uL]</i>	pJRK28	
CX7762	<i>cwn-2(ok895) IV; kyEx1183[myo-3::cwn-2, 100ng/uL, odr-1::RFP 50ng/uL]</i>	pJRK21	
CX8381	<i>cwn-2(ok895) IV; kyEx1369[hsp-16.41::cwn-2, 100ng/uL, odr-1::RFP 50ng/uL]</i>	pJRK23	
CX10087	<i>cam-1(gm122) II; gmls18 X; kyEx2285[pSP50 60ng/uL, ofm-1::dsRED 25ng/uL]</i>	pSP50	Francis et al., 2005
CX10088	<i>cam-1(gm122) II; gmls18 X; kyEx2286[pDM109, 50ng/uL, odr-1::RFP 30ng/uL]</i>	pDM109	Francis et al., 2005
CX10464	<i>cam-1(gm122) II; gmls18 X; kyEx2541[cam-1A::cam-1A, 1ng/uL, odr-1::RFP 50ng/uL]</i>	pJRK76	
CX10454	<i>cam-1(gm122) II; gmls18 X; kyEx2533[cam-1B::cam-1B, 1ng/uL, odr-1::RFP 50ng/uL]</i>	pJRK80	
CX10449	<i>cam-1(gm122) II; gmls18 X; kyEx2531[cam-1C::cam-1C, 5ng/uL, odr-1::RFP 50ng/uL]</i>	pJRK84	
CX10478	<i>cam-1(gm122) II; gmls18 X; kyEx2543[cam-1A::cam-1C, 1ng/uL, odr-1::RFP 50ng/uL]</i>	pJRK78	
CX10477	<i>cam-1(gm122) II; gmls18 X; kyEx2542[unc-119::cam-1A, 1ng/uL, ofm-1::dsRED 25ng/uL]</i>	pJRK97	
CX10797	<i>cam-1(gm122) II; gmls18 X; kyEx2765[ceh-24::cam-1A, 20ng/uL, ofm-1::dsRED 25ng/uL]</i>	pJRK102	
CX11010	<i>cam-1(gm122) II; gmls18 X; kyEx2881[mig-1::cam-1A, 20ng/uL, ofm-1::dsRED 25ng/uL]</i>	pJRK101	
CX10999	<i>cam-1(gm122) II; gmls18 X; kyEx2877[cwn-2::cam-1A, 1ng/uL, ofm-1::dsRED 25ng/uL]</i>	pJRK103	
CX11000	<i>cam-1(gm122) II; gmls18 X; kyEx2878[cwn-2::cam-1A, 1ng/uL, ofm-1::dsRED 25ng/uL]</i>	pJRK103	
CX10898	<i>cam-1(gm122) II; gmls18 X; kyEx2815[nsy-5::cam-1A, 5ng/uL, ofm-1::dsRED 25ng/uL]</i>	pJRK96	
CX10948	<i>cam-1(gm122) II; gmls18 X; kyEx2849[ncs-1::cam-1A, 5ng/uL, ofm-1::dsRED 25ng/uL]</i>	pJRK98	
CX10855	<i>kyEx2796[ceh-24::GFP, 20ng/uL, odr-1::RFP 50ng/uL]</i>	pJRK105	
CX12132	<i>mig-1(e1787) I; kyEx2796[ceh-24::GFP, 20ng/uL, odr-1::RFP 50ng/uL]</i>	pJRK105	
CX11171	<i>cfz-2(ok1201) V; kyEx2796[ceh-24::GFP, 20ng/uL, odr-1::RFP 50ng/uL]</i>	pJRK105	
CX11101	<i>cam-1(gm122) II; kyEx2796[ceh-24::GFP, 20ng/uL, odr-1::RFP 50ng/uL]</i>	pJRK105	
CX10858	<i>sax-3(ky123) gmls18 X; kyEx2797[ceh-24::sax-3, 20ng/uL, ofm-1::dsRED 25ng/uL]</i>	pJRK119	
CX10909	<i>sax-3(ky123) gmls18 X; kyEx2822[ceh-24::sax-3, 20ng/uL, ofm-1::dsRED 25ng/uL]</i>	pJRK119	
CX12031	<i>ced-3(n717) IV; kyEx3294[ceh-24::egl-1, 2.5ng/uL, pSM, 25ng/uL, elt-2::mcherry, 1ng/uL]</i>	pJRK134	
CX12665	<i>cwn-2(ky756) ced-3(n717) IV; kyEx3294[ceh-24::egl-1, 2.5ng/uL, pSM, 25ng/uL, elt-2::mcherry, 1ng/uL]</i>	pJRK134	
CX12206	<i>mig-1(e1787) I; cam-1(gm122) II; gmls18 X; kyEx2285[pSP50 60ng/uL, ofm-1::dsRED 25ng/uL]</i>	pSP50	Francis et al., 2005
CX12668	<i>mig-1(e1787) I; cam-1(ks52) II; kyEx3400 [ceh-24::mig-1A 5ng/uL, ofm-1::dsRED 25ng/uL]</i>	pJRK135	
CX10483	<i>cam-1(gm122) II; sax-3(ky200) gmls18 X; kyEx2285[pSP50 60ng/uL, ofm-1::dsRED 25ng/uL]</i>	pSP50	Francis et al., 2005
CX11126	<i>cfz-2(ok1201) V; gmls18 X; kyEx2940[ceh-24::cfz-2 20ng/uL, ofm-1::dsRED, 25ng/uL]</i>	pJRK129	
CX11125	<i>cfz-2(ok1201) V; gmls18 X; kyEx2939[ceh-24::cfz-2 20ng/uL, ofm-1::dsRED, 25ng/uL]</i>	pJRK129	
CX12667	<i>kyls510 II; kyEx3399 [cam-1A::mCherry, 50ng/uL]</i>	pJRK85	
CX12666	<i>kyls510 II; cwn-2(ky756) IV; kyEx3398 [cam-1A::mCherry, 50ng/uL]</i>	pJRK85	
CX11133	<i>kyEx2942[mig-1::myrGFP, 20ng/uL, ofm-1::dsRED 25ng/uL]</i>	pJRK109	
CX11186	<i>cwn-2(ky756) IV; kyEx2942[mig-1::myrGFP, 20ng/uL, ofm-1::myrGFP, 25ng/uL]</i>	pJRK109	
CX10878	<i>kyls510 II</i>	pJRK106	
NG3146	<i>gmls18 X</i>	pTF1	Lai and Garriga, 2004
CX6232	<i>slt-1(eh15) gmls18 X</i>		
CX6654	<i>sax-3(ky200) gmls18 X</i>		
CX7134	<i>cwn-2(ky736) IV; gmls18 X</i>		
CX7135	<i>cwn-2(ky756) IV; gmls18 X</i>		
CX7192	<i>cwn-2(ok895) IV; gmls18 X</i>		
CX7715	<i>cam-1(gm122) II; gmls18 X</i>		
CX8224	<i>cfz-2(ok1201) V; gmls18 X</i>		
CX8245	<i>lin-17(n677) I; gmls18 X</i>		
CX8244	<i>lin-18(e620) gmls18 X</i>		
CX9175	<i>mig-1(e1787) I; gmls18 X</i>		
CX7615	<i>cam-1(gm122) II; cwn-2(ky756) IV; gmls18 X</i>		
CX8266	<i>cfz-2(ok1201) V; cwn-2(ky756) IV; gmls18 X</i>		
CX8505	<i>cfz-2(ok1201) V; cam-1(gm122) II; gmls18 X</i>		
CX8929	<i>lin-17(n677) I; cfz-2(ok1201) V; gmls18 X</i>		
CX9169	<i>mig-1(e1787) I; cfz-2(ok1201) V; gmls18 X</i>		
CX9168	<i>mig-1(e1787) I; cam-1(gm122) II; gmls18 X</i>		
CX9474	<i>cwn-1(ok546) II; gmls18 X</i>		
CX9674	<i>lin-44(n1792) I; gmls18 X</i>		
CX9366	<i>lin-44(n1792) I; cwn-1(ok546) II; gmls18 X</i>		
CX9681	<i>lin-44(n1792) I; cwn-2(ky756) IV; gmls18 X</i>		
CX9130	<i>cwn-1(ok546) II; cwn-2(ky756) IV; gmls18 X</i>		
CX10068	<i>lin-44(n1792) I; cwn-1(ok546) II; egl-20(n585) IV; gmls18 X</i>		
CX8717	<i>cam-1(ks52) II; gmls18 X</i>		
CX10871	<i>mig-1(e1787) I; cam-1(ks52) II; gmls18 X</i>		
CX11032	<i>mig-13(mu225) gmls18 X</i>		
CX11093	<i>cam-1(ks52) II; mig-13(mu225) gmls18 X</i>		
CX10129	<i>cam-1(ks52) II; sax-3(ky200) gmls18 X</i>		
CX10897	<i>cam-1(ks52) II; cfz-2(ok1201) V; gmls18 X</i>		
CX12669	<i>lin-17(n677) I; cam-1(ks52) II; gmls18 X</i>		
CX8908	<i>cam-1(ks52) II; lin-18(e620) gmls18 X</i>		
EU452	<i>mom-5(zu193) unc-13(e1091) / hT2 I; + / hT2[bli-4(e937) let-? (h661)] III</i>		
CX10479	<i>cam-1(gm122) II; sax-3(ky200) gmls18 X</i>		
MT1522	<i>ced-3(n717) IV</i>		
CX7424	<i>cwn-2(ky756) IV; akIs3[nmr-1::GFP] V</i>		
VM484	<i>akIs3[nmr-1::GFP] V</i>		

Reference
Lai, T. and Garriga, G. (2004). The conserved kinase UNC-51 acts with VAB-8 and UNC-14 to regulate axon outgrowth in *C. elegans*. *Development* **131**, 5991-6000.

Table S3. Primary data from transgenic rescue experiments demonstrating rescue or absence of rescue of *cwn-2* (top), *cam-1* (middle) and *cfz-2* (bottom)

	Background	Penetrance (%)	Anterior nerve ring (n)	Normal nerve ring (n)	Total (n)
<i>cwn-2</i> rescue experiments					
<i>cwn-2</i> genomic	With transgene	0.0	0	48	48
	Without transgene	14.9	7	40	47
<i>myo-3::cwn-2</i>	With transgene	0.0	0	26	26
	Without transgene	54.3	25	21	46
<i>myo-2::cwn-2</i>	With transgene	7.1	5	65	70
	Without transgene	70.4	50	21	71
<i>elt-2::cwn-2</i>	With transgene	10.0	1	9	10
	Without transgene	83.3	15	3	18
<i>slt-1::cwn-2</i>	With transgene	0.0	0	27	27
	Without transgene	48.4	15	16	31
<i>cam-1</i> rescue experiments					
<i>cam-1</i> genomic DNA (pDM109)	With transgene	1.1	1	87	88
	Without transgene	15.8	3	16	19
<i>cam-1A::cam-1A</i>	With transgene	6.3	4	59	63
	Without transgene	42.9	9	12	21
<i>cam-1B::cam-1B</i>	With transgene	20.3	14	55	69
	Without transgene	51.1	23	22	45
<i>cam-1C::cam-1C</i>	With transgene	23.8	20	64	84
	Without transgene	20.0	9	36	45
<i>cam-1A::cam-1C</i>	With transgene	13.6	9	57	66
	Without transgene	41.9	49	68	117
<i>unc-119::cam-1A</i>	With transgene	3.8	2	51	53
	Without transgene	36.8	21	36	57
<i>ceh-24::cam-1A</i>	With transgene	11.3	6	47	53
	Without transgene	42.7	35	47	82
<i>cwn-2::cam-1A</i>	With transgene	27.9	17	44	61
	Without transgene	30.2	16	37	53
<i>mig-1::cam-1A</i>	With transgene	7.9	3	35	38
	Without transgene	22.7	15	51	66
<i>nsy-5::cam-1A</i>	With transgene	23.9	21	67	88
	Without transgene	32.8	41	84	125
<i>ncs-1::cam-1A</i>	With transgene	37.7	29	48	77
	Without transgene	30.8	32	72	104
<i>opt-3::cam-1A</i>	With transgene	44.1	15	19	34
	Without transgene	29.4	15	36	51
<i>cfz-2</i> rescue experiments					
<i>ceh-24::cfz-2</i> line 1	With transgene	30.6	19	43	62
	Without transgene	17.8	18	83	101
<i>ceh-24::cfz-2</i> line 2	With transgene	26.5	18	50	68
	Without transgene	17.5	11	52	63

For presentation in Fig. 3D and Fig. 6B, the data were normalized such that the defects in the animals without the transgene were comparable for all genotypes (100%). See Materials and methods for details.

Table S4. Plasmids used

Plasmid	Description	Promoter and coding region	Vector
pSM	Modified Fire Vector	Contains <i>FseI</i> and <i>Ascl</i> sites for cloning promoters, and <i>NheI</i> and <i>SacI</i> sites for cloning <i>cam-1</i> cDNAs	
pJG7	Modified Fire Vector	Contains <i>FseI</i> and <i>Ascl</i> sites for cloning promoters and <i>SmaI</i> site for genomic fragments, and an SL2::GFP sequence for monitoring expression	
pJG13	Modified Fire Vector	Contains <i>FseI</i> and <i>Ascl</i> sites for cloning promoters, <i>NheI</i> and <i>SacI</i> sites for cloning <i>cam-1</i> cDNA, <i>KpnI</i> and <i>SacI</i> sites for cloning <i>cwn-2</i> cDNA, and an SL2::CFP sequence for monitoring expression	
pSM-GFP	Modified Fire Vector	Contains <i>FseI</i> and <i>Ascl</i> sites for cloning promoters, a synthetic intron, then GFP	
pSM-cherry	Modified Fire Vector	Contains <i>FseI</i> and <i>Ascl</i> sites for cloning promoters, a synthetic intron, then mCherry	
pSM-myrGFP	Modified Fire Vector	Contains <i>FseI</i> and <i>Ascl</i> sites for cloning promoters, a synthetic intron, then myristoylated GFP cDNA	
pJRK20	<i>cwn-2</i> genomic	W01B6 genomic fragment from <i>AfIII</i> to <i>FauI</i>	pJG7
pJRK23	<i>hsp-16.41::cwn-2</i>	Heat-shock promoter:: <i>cwn-2</i> cDNA	pPD49.83
pJRK22	<i>myo-2::cwn-2</i>	<i>myo-2</i> promoter:: <i>cwn-2</i> cDNA (<i>NheI</i> and <i>SacI</i> sites)	pPD30.69
pJRK21	<i>myo-3::cwn-2</i>	<i>myo-3</i> promoter:: <i>cwn-2</i> cDNA (<i>KpnI</i> and <i>SacI</i> sites)	pPD96.52
pJRK27	<i>elt-2::cwn-2</i>	5 kb upstream of <i>elt-2</i> ATG and <i>cwn-2</i> cDNA	pJG13
pJRK28	<i>slt-1::cwn-2</i>	4 kb upstream of <i>slt-1</i> ATG and <i>cwn-2</i> cDNA	pJG13
pJRK76	<i>cam-1A::cam-1A</i>	7.8 kb upstream of <i>cam-1A</i> ATG and <i>cam-1A</i> cDNA	pSM
pJRK80	<i>cam-1B::cam-1B</i>	5.4 kb upstream of <i>cam-1B</i> ATG and <i>cam-1B</i> cDNA	pSM
pJRK84	<i>cam-1C::cam-1C</i>	5.1 kb upstream of <i>cam-1C</i> ATG and <i>cam-1C</i> cDNA	pSM
pJRK78	<i>cam-1A::cam-1C</i>	7.8 kb upstream of <i>cam-1A</i> ATG and <i>cam-1C</i> cDNA	pSM
pJRK97	<i>unc-119::cam-1A</i>	2.2 kb upstream of <i>unc-119</i> ATG and <i>cam-1A</i> cDNA	pJG13
pJRK102	<i>ceh-24::cam-1A</i>	2.9 kb upstream of <i>ceh-24</i> ATG and <i>cam-1A</i> cDNA	pJG13
pJRK101	<i>mig-1::cam-1A</i>	6.5 kb upstream of <i>mig-1</i> ATG and <i>cam-1A</i> cDNA	pJG13
pJRK103	<i>cwn-2::cam-1A</i>	3.4 kb upstream of <i>cwn-2</i> ATG and <i>cam-1A</i> cDNA	pSM
pJRK96	<i>nsy-5::cam-1A</i>	5.6 kb upstream of <i>nsy-5</i> ATG and <i>cam-1A</i> cDNA	pJG13
pJRK100	<i>opt-3::cam-1A</i>	2.5 kb upstream of <i>opt-3</i> ATG and <i>cam-1A</i> cDNA	pSM
pJRK98	<i>ncs-1::cam-1A</i>	2.1 kb upstream of <i>ncs-1</i> ATG and <i>cam-1A</i> cDNA	pSM
pJRK119	<i>ceh-24::sax-3</i>	2.9 kb upstream of <i>ceh-24</i> ATG and <i>cam-1A</i> cDNA	pJG13
pJRK105	<i>ceh-24::GFP</i>	2.9 kb upstream of <i>ceh-24</i> ATG and GFP cDNA	pSM-GFP
pSP50	<i>cam-1</i> N-terminal deletion	<i>cam-1</i> genomic DNA with deletion of N-terminal cytoplasmic domain (Francis et al., 2005)	
pDM109	<i>cam-1</i> genomic::GFP	<i>cam-1</i> genomic DNA with N-terminal GFP fusion (Francis et al., 2005)	
pJRK135	<i>ceh-24::mig-1A</i>	2.9 kb upstream of <i>ceh-24</i> ATG and <i>mig-1A</i> cDNA	pSM
pJRK134	<i>ceh-24::egl-1</i>	2.9 kb upstream of <i>ceh-24</i> ATG and <i>egl-1</i> cDNA	pSM
pJRK106	<i>ceh-24::myrGFP</i>	2.9 kb upstream of <i>ceh-24</i> ATG and myristoylated GFP cDNA	pSM-myrGFP
pJRK129	<i>ceh-24::cfz-2</i>	2.9 kb upstream of <i>ceh-24</i> ATG and <i>cfz-2</i> cDNA	pSM
pJRK85	<i>cam-1A::mCherry</i>	7.8 kb upstream of <i>cam-1A</i> ATG and mCherry cDNA	pSM-cherry
pJRK109	<i>mig-1::myrGFP</i>	6.5 kb upstream of <i>mig-1</i> ATG and myristoylated GFP cDNA	pSM-myrGFP

pPD vectors generated by A. Fire and colleagues are described in Fire et al. (1990). Some *cam-1* clones are described in Francis et al. (2005).

References

Fire, A., Harrison, S. W. and Dixon, D. (1990). A modular set of lacZ fusion vectors for studying gene expression in *Caenorhabditis elegans*. *Gene* **93**, 189-198.
Francis, M. M., Evans, S. P., Jensen, M., Madsen, D. M., Mancuso, J., Norman, K. R. and Maricq, A. V. (2005). The Ror receptor tyrosine kinase CAM-1 is required for ACR-16-mediated synaptic transmission at the *C. elegans* neuromuscular junction. *Neuron* **46**, 581-594.

Axon Guidance defects in SIA/SIB/SMD neurons

	No defect (%)	Anterior axon directly from ganglion (%)	Anterior axon from nerve ring (%)	Anterior axon from posterior (%)	n
<i>wt</i>	94.8	3.4	0	1.7	58
<i>mig-1(e1787)</i>	95.8	1.1	0	3.1	95
<i>cfz-2(ok1201)</i>	83	11.3	0	7.5	53
<i>cam-1(gm122)</i>	28.1	38.6	40.4	14	57
<i>cwn-2(ky756)</i>	40.6	43.8	12.5	17.1	64



Supplemental Table 2